THE FASEB JOURNAL • RESEARCH • www.fasebj.org

The classic metal-sensing transcription factor MTF1 promotes myogenesis in response to copper

Cristina Tavera-Montañez,*[,1] Sarah J. Hainer,[†,1,2] Daniella Cangussu,* Shellaina J. V. Gordon,* Yao Xiao,[‡] Pablo Reyes-Gutierrez,* Anthony N. Imbalzano,* Juan G. Navea,[‡] Thomas G. Fazzio,[†] and Teresita Padilla-Benavides*[,3]

*Department of Biochemistry and Molecular Pharmacology, [†]Department of Molecular, Cell, and Cancer Biology, University of Massachusetts Medical School, Worcester, Massachusetts, USA; and [‡]Department of Chemistry, Skidmore College, Saratoga Springs, New York, USA

ABSTRACT: Metal-regulatory transcription factor 1 (MTF1) is a conserved metal-binding transcription factor in eukaryotes that binds to conserved DNA sequence motifs, termed metal response elements. MTF1 responds to both metal excess and deprivation, protects cells from oxidative and hypoxic stresses, and is required for embryonic development in vertebrates. To examine the role for MTF1 in cell differentiation, we use multiple experimental strategies [including gene knockdown (KD) mediated by small hairpin RNA and clustered regularly interspaced short palindromic repeats/CRISPR-associated protein 9 (CRISPR/Cas9), immunofluorescence, chromatin immunopreciptation sequencing, subcellular fractionation, and atomic absorbance spectroscopy] and report a previously unappreciated role for MTF1 and copper (Cu) in cell differentiation. Upon initiation of myogenesis from primary myoblasts, both MTF1 expression and nuclear localization increased. *Mtf1* KD impaired differentiation, whereas addition of nontoxic concentrations of Cu^+-enhanced MTF1 expression and promoted myogenesis. Furthermore, we observed that Cu^+ binds stoichiometrically to a C terminus tetra-cysteine of MTF1. MTF1 bound to chromatin at the promoter regions of myogenic genes, and Cu addition stimulated this binding. Of note, MTF1 formed a complex with myogenic differentiation (MYOD)1, the master transcriptional regulator of the myogenic lineage, at myogenic promoters. These findings uncover unexpected mechanisms by which Cu and MTF1 regulate gene expression during myoblast differentiation.—Tavera-Montañez, C., Hainer, S. J., Cangussu, D., Gordon, S. J. V., Xiao, Y., Reyes-Gutierrez, P., Imbalzano, A. N., Navea, J. G., Fazzio, T. G., Padilla-Benavides, T. The classic metal-sensing transcription factor MTF1 promotes myogenesis in response to copper. FASEB J. 33, 000–000 (2019). www.fasebj.org

KEY WORDS: myogenic differentiation 1 · ChIP-Seq · copper binding

Copper (Cu) is an essential micronutrient required for human development and function. Cu plays a role in several key cellular functions, such as respiration, antioxidant defense, neurotransmitter biogenesis, disproportionation of O^-, and metal ion homeostasis (1–3). Dysregulation of cellular Cu levels is detrimental to human health, and it is associated with redox stress, disruption of iron-sulfur cluster proteins, lipid peroxidation, and DNA oxidation (4). Consequently, cells must control Cu levels and prevent accumulation of labile Cu in the cytosol. Cu homeostasis is maintained by a complex cellular network of transmembrane transport systems, soluble chaperones, chelating proteins, and transcription factors (TFs) (3, 5–8). Cu depletion or overload leads to pathologic conditions, such as Menkes disease and Wilson disease, respectively (8–15). Menkes disease is characterized by severe Cu deficiency due to mutations in the Cu^+-ATPase ATP7A that disrupt dietary Cu absorption. These inactivating mutations result in neurologic abnormalities, blood vessel and connective tissue defects, and weak muscle

ABBREVIATIONS: AAS, atomic absorbance spectroscopy; ATOX, antioxidant 1 copper chaperone; Cas9, CRISPR-associated protein 9; Cd, cadmium; ChIP, chromatin immunoprecipitation; ChIP-Seq, chromatin immunoprecipitation sequencing; CRISPR, clustered regularly interspaced short palindromic repeats; Cu, copper; FBS, fetal bovine serum; GO, gene ontology; GST, glutathione *S*-transferase; HRP, horseradish peroxidase; IHC, immunohistochemistry; IP, immunoprecipitation; KD, knockdown; MBS, Cu^+-binding site; MRE, metal-responsive element; MT, metallothionein; *Mt1*, Metallothionein 1; MTF1, metal-regulatory transcription factor 1; MYOD, myogenic differentiation; Pax7, Paired box protein 7; PBT, phosphate-buffered triton; qPCR, quantitative PCR; qRT-PCR, quantitative RT-PCR; *scr*, scramble; SERCA, sarco/endoplasmic reticulum Ca^{2+}-ATPase; sgRNA, single guide RNA; shRNA, small hairpin RNA; SOD, superoxide dismutase; TEPA, tetraethylenepentamine; TF, transcription factor; TSS, transcriptional start site; WT, wild type; Zn, zinc

[1] These authors contributed equally to this work.

[2] Current affiliation: Department of Biological Sciences, University of Pittsburgh, Pittsburgh, PA, USA.

[3] Correspondence: Department of Biochemistry and Molecular Pharmacology, University of Massachusetts Medical School, 364 Plantation St., Worcester, MA 01605, USA. E-mail: teresita.padilla@umassmed.edu

doi: 10.1096/fj.201901606R

This article includes supplemental data. Please visit *http://www.fasebj.org* to obtain this information.

tone (hypotonia) (16–20). Wilson disease, which arises from mutations in the Cu^+-ATPase ATP7B, results in Cu accumulation in the liver, brain, and eyes (19, 21, 22). This Cu overload leads to a variety of hepatic and neurologic defects, cardiomyopathies, and muscular abnormalities, such as a lack in coordination (ataxia) and repetitive movements (dystonia) (23, 24).

Cu is a fundamental cofactor for several enzymes, including cytochrome *c* oxidase, and superoxide dismutases (SOD1 and SOD3) (1, 2). Cu is also an important component of enzymes that contribute to proper tissue function (25–28). Myogenesis encompasses several metabolic and morphologic changes that are linked to Cu^+-dependent cellular energy production and redox homeostasis (1, 2, 29). Satellite cells, which are adult stem cells that promote skeletal muscle growth and repair, have specific bioenergetic demands when undergoing transition from quiescence to proliferation and differentiation. The transition from quiescence to proliferation is accompanied by a metabolic switch from fatty acid oxidation to glycolysis, which modulates epigenetic and transcriptional changes (30). During myoblast differentiation, a metabolic shift occurs in which energy is produced *via* oxidative phosphorylation, a process largely dependent on Cu bioavailability (31, 32). This metabolic shift involves the coordinated expression of nuclear and mitochondrial genomes, which leads to an increase in the production of mitochondria and associated cuproenzymes essential for energy production *via* oxidative phosphorylation (*e.g.*, cytochrome *c* oxidase) and redox homeostasis (*e.g.*, SOD1) (1, 2, 32–34).

We recently demonstrated that Cu is required for the proliferation and differentiation of primary myoblasts derived from mouse satellite cells (35). During myogenesis, the cellular levels of Cu increased, which is consistent with a high demand for Cu for proper function of mature tissue (35). These changes in Cu levels are dependent on the dynamic expression of the Cu^+-transporters and the posttranscriptional regulation of *Atp7a* (35). However, the mechanisms by which Cu elicits a differentiation effect are unknown. Here, we hypothesized that Cu may have a fundamental role in the regulation of gene expression that drives differentiation of skeletal muscle. Activation of the myogenic program at the transcriptional level requires a series of signals, including growth factors, TFs, kinases, chromatin remodelers, histone modifiers, and metal ions (35–51). Emerging evidence suggests that Cu and potential Cu^+-binding TFs play significant roles in mammalian development (52–55). Despite this, only 3 Cu^+-binding factors are known to regulate gene expression in mammalian cells, and little is known about their roles in developmental processes (52, 53, 56–65).

Metal-regulatory transcription factor 1 (MTF1) is a highly conserved zinc (Zn)-binding TF that recognizes and binds metal-responsive elements (MREs) to promote the transcription of genes that maintain metal homeostasis (56, 58, 60, 66–69). MREs are characterized by the -TGCRCNC- consensus sequence located near the promoters of genes related to redox and metal homeostasis (70–72). MTF1 transcriptional activity is associated with the availability of Zn ions (73); however, the molecular mechanisms by which metals activate MTF1 remain unclear. Current models for MTF1 activation include: *1*) stimulation by free cytosolic Zn; *2*) interaction with Zn released from metallothioneins (MTs); or *3*) MTF1 phosphorylation/dephosphorylation (72, 74–78). Under normal conditions, MTF1 is primarily located in the cytoplasm. When MTF1 is activated, it translocates from the cytoplasm to the nucleus, where it recognizes and interacts with MREs of genes that mediate homeostasis (60, 66, 79–84). Chromatin immunoprecipitation (ChIP) analysis of *Drosophila* MTF1 has shown that different metal stimuli (Cu and Cd) result in variations in the recognition of single nucleotides in genomic DNA sequences, demonstrating that binding specificity can be altered by the presence of different metals (85). *Drosophila* MTF1 has a Cu^+ sensing function that is mediated in part by a carboxy-terminal tetra-nuclear Cu^+ cluster (86). A similar Cu^+-binding center has been identified in mammalian MTF1, suggesting that it may also respond to Cu (86). Whether this response is associated with maintenance of metal homeostasis, or if it is related to other cellular functions, remains unexplored.

In this study, we found that MTF1 is induced and translocated to the nucleus upon initiation of myogenesis in primary myoblasts derived from mouse satellite cells. Small hairpin RNA (shRNA) and clustered regularly interspaced short palindromic repeats/CRISPR-associated protein 9 (CRISPR/Cas9)-mediated depletion of *Mtf1* causes lethality of differentiating myoblasts, indicating that MTF1 is essential for myogenesis. Nuclear levels of Cu increase in differentiating primary myoblasts and significantly decrease upon partial deletion of *Mtf1*. *In vitro* characterization of the murine MTF1 carboxy-terminal binding domain determined it bound stoichiometrically to Cu^+. Chromatin immunoprecipitation sequencing (ChIP-Seq) and ChIP–quantitative PCR (qPCR) localization analyses revealed novel MTF1 target genes that are associated with myogenesis in addition to classic metal homeostasis genes. MTF1 interaction with myogenic genes is enhanced by supplementation of nontoxic concentrations of Cu to the myoblast differentiation medium. Finally, our data indicate that 1 potential mechanism by which MTF1 participates in transcriptional regulation of myogenic genes is through an interaction with myogenic differentiation (MYOD). Expression of exogenous wild-type (WT) MTF1 rescues the differentiation phenotype observed in *Mtf1* knockdown (KD) primary myoblasts. However, complementation with MTF1 mutated in the tetra-nuclear cysteine cluster resulted in delayed differentiation. Taken together, our results shed light on the underappreciated role of Cu and Cu-binding TFs in the development of skeletal muscle.

MATERIALS AND METHODS

Primary cell culture

Mouse satellite cells were isolated from leg muscle of 3–6-wk-old WT C57Bl/6 mice. The muscle was extracted and cut into small pieces, washed with HBSS (Thermo Fisher Scientific, Waltham,

MA, USA) and incubated with 0.1% Pronase for 1 h at 37°C. The cells were then filtered using a 100-μm cell sieve and resuspended in 3 ml of growth medium [1:1 v/v DMEM:F-12, 20% fetal bovine serum (FBS), and 25 ng/ml of basic fibroblast growth factor (FGF) FGF]. Cells were filtered again using a 40-μm cell sieve and centrifuged at 1000 *g* for 1 min at room temperature. The cells were placed at the top of a Percoll step-gradient (35 and 70%) and centrifuged 20 min at 1850 *g* at room temperature. The myoblasts were contained in the lower interface of the 70% Percoll fraction and were washed with HBSS, centrifuged 5 min at 1000 *g*, and resuspended in growth medium for plating. Myoblasts were grown and differentiated on plates coated with 0.02% collagen (Advanced BioMatrix, Carlsbad, CA, USA) (87). The different treatments (indicated in the figures) were as follows: Proliferation and differentiation (24 h): the differentiation medium was supplemented or not with insulin because it is necessary to induce myogenesis *via* signaling cascades such as the PI3K and FAK pathways (88, 89). Presence and absence of $CuSO_4$ or tetraethylenepentamine (TEPA): the concentrations used were 100 μM for proliferating cells and 30 μM for differentiating cells as previously described by Vest *et al.* (35). To test the effect of Cu and MTF1 in myogenesis, we eliminated insulin from the differentiation medium from the Cu-treated cells as previously described by Vest *et al.* (35) because this condition partially inhibits myogenesis.

Plasmid construction, virus production, and transduction of primary myoblasts

MTF1 WT pET-glutathione *S*-transferase (GST)/tobacco etch virus (TEV)/murine MTF1 (mMtf1)[NM_008636.4] plasmid was purchased from VectorBuilder (Chicago, IL, USA). This plasmid was used as a template to introduce the mutations coding for the multiple Alanine substitutions in the putative carboxy-terminus Cu^+-binding site (MBS) using the oligos indicated in Supplemental Table S5. Mutations were introduced using the Quik Change mutagenesis kit following the manufacturer's instructions (Agilent Technologies, Santa Clara, CA, USA). The pET vector places a GST tag at the amino terminus, which was used for purification of the recombinant proteins. DNA sequences were confirmed by automated sequencing.

For shRNA viral production, Mission plasmids (MilliporeSigma, Burlington, MA, USA) encoding for 2 different shRNA against *Mtf1* and a scramble (*scr*) are indicated in Supplemental Table S4. CRISPR/Cas9 plasmid construction was performed by 4 custom-designed single guide RNAs (sgRNAs) to recognize the intron/exon junctions 1, 2, 3, and 4 of *Mtf1* mouse gene (reference sequence: NM_008636.4). Each sgRNA consisted of 20 nt complementary to the sequence that precedes a 5′-NGG protospacer-adjacent motif located in the targeted intron/exon junctions. Specificity was validated by search through the entire genome to avoid off-target effects. Preparation of CRISPR/Cas9 lentiviral constructs was performed using the lentiCRISPRv2 oligo cloning protocol (90). Briefly, sense and antisense oligos obtained from Integrated DNA Technology (Coralville, IA, USA) were set according to the designed sgRNA and were annealed and phosphorylated to form double-stranded oligos. Subsequently, they were cloned into the BsmBI–BsmBI sites downstream from the human U6 promoter of the lentiCRISPRv2 plasmid (90, 91) that was a kind gift from Dr. Feng Zhang (plasmid 52961; Addgene, Cambridge, MA, USA). The empty plasmid that expresses only Cas9 but no sgRNA was included as null knockout control. Oligonucleotides used to form double-stranded sgRNAs are listed in Supplemental Table S5. To generate the retroviral constructs for MTF1 WT and the MBS mutant to recover expression, the coding sequence of MTF1 or MBS mutant with addition of a C-terminal FLAG tag sequence was PCR amplified from the pET vectors used for expression of MTF1 in bacteria. PCR products were subsequently cloned into the pBABE retroviral vector containing a blasticidin resistance gene (92). All constructs were confirmed by sequencing. Primers used are included in Supplemental Table S4. To generate lentiviral particles, 5×10^6 HEK293T cells were plated in 10-cm dishes. The next day, transfection was performed using 15 μg of either each shRNA constructs or sgRNA-containing CRISPR/CAS9 constructs mixed with the packing vectors pLP1 (15 μg), pLP2 (6 μg), and vesicular stomatitis virus glycoprotein plasmid (pVSBG) pSVGV (3 μg). Retrovirus production was performed using 15 μg of retroviral constructs expressing either MTF1 WT or MBS mutant transfected in BOSC23 cells (93). Transfections were performed using Lipofectamine 2000 according to the manufacturer's instructions (Thermo Fisher Scientific). The medium was changed the next day to 10 ml DMEM with 10% FBS (Thermo Fisher Scientific). The viral supernatant was harvested after 48 h of incubation and filtered through a 0.45-μm syringe filter (MilliporeSigma). To infect primary myoblasts, 5 ml of the filtered supernatant supplemented with 8 μg/ml polybrene (MilliporeSigma) were used to infect 2 million cells. After overnight incubation, infected cells were then selected in DMEM/F12 (Thermo Fisher Scientific) containing 20% FBS as well as 0.75 ng/ml of FGF containing 1.5 μg/ml puromycin or 5 μg/ml blasticidin (Thermo Fisher Scientific).

Antibodies

Primary antibodies (used at 1:1000) were obtained from Santa Cruz Biotechnology (Dallas, TX, USA): rabbit anti-MTF1 (sc-365090), rabbit anti-PI3K (sc-515646), mouse anti–sarco/endoplasmic reticulum Ca^{2+}-ATPase (SERCA) (sc-271669), mouse anti-RNA Polymerase II (sc-55492) and rabbit anti-ATP7A (H-180, sc-32900). From ABclonal (Woburn, MA, USA): rabbit anti–caspase-3 (A2156), rabbit anti-SOD1 (A0274), rabbit anti-Flag (AE005), rabbit anti-ATOX1 (A6874), rabbit anti-MYOD (A0671) and mouse anti–β-tubulin (AC021). The rabbit anti–glyceraldehyde 3-phosphate dehydrogenase (GAPDH)-HRP was from MilliporeSigma (G9295). Normal rabbit IgG was obtained from Cell Signaling Technology (2729; Danvers, MA, USA). The anti–myosin heavy chain (MF20, deposited by D. A. Fischman, Department of Anatomy and Cell Biology, State University of New York, Brooklyn, NY, USA), antimyogenin antibody (F5D, deposited by W. E. Wright, Department of Cell Biology and Neuroscience, University of Texas Southwestern Medical School, Dallas, TX, USA) was obtained as hybridoma supernatants from the Developmental Studies Hybridoma Bank (The University of Iowa, Iowa City, IA, USA). The secondary antibodies used were goat anti-rabbit and anti-mouse coupled to HRP (1:1000; Thermo Fisher Scientific).

Primary myoblast immunofluorescence

Primary myoblasts for immunofluorescence were grown on glass bottom Cellview Advanced TC culture dishes (Grenier Bio-One, Monroe, NC, USA). Samples were obtained for proliferation and at 24, 48, and 72 h after induction of differentiation. Cells were fixed in 10% formalin, permeabilized with phosphate-buffered triton (PBT) buffer (0.5% Triton X-100 in PBS) and blocked in 5% horse serum in PBT. Cells were incubated with the rabbit anti-MTF1 or anti-FLAG antibodies (1:100) in blocking solution overnight at 4°C. The samples were then washed 3 times with PBT solution for 10 min at room temperature. Then, the cells were incubated with the goat anti-rabbit Alexa-488 secondary antibody (1:500; Thermo Fisher Scientific) in blocking solution for 2 h at room temperature and 30 min with DAPI. Cells were counterstained with DAPI and imaged with a Leica TCS SP5

Confocal Laser Scanning Microscope (Leica Microsystems, Buffalo Grove, IL, USA) using a ×40 water immersion objective.

Immunohistochemistry

Proliferating and differentiating primary myoblasts at the desired time points were fixed overnight in 10% formalin-PBS at 4°C. Samples were washed with PBS and permeabilized for 10 min in PBS containing 0.2% Triton X-100. Immunohistochemistry (IHC) was performed using Universal ABC Kit and developed with Vectastain Elite ABC HRP Kit (both from Vector Laboratories, Burlingame, CA, USA) following the manufacturer's instructions.

Calculation of fusion index for the myotubes

The fusion index was calculated as the ratio of the nuclei number in myocytes with 2 or more nuclei *vs.* the total number of nuclei. Edges and regions that did not show good cell adhesion were not used for analysis. Three independent biologic replicates were grown in 48-well plates and cells were induced to differentiate as described above. Three patterns on each dish were used for quantitative analysis using ImageJ software v.1.8 (National Institutes of Health, Bethesda, MD, USA).

Gene expression analyses

Three independent biologic replicates of proliferating and differentiating (24 h) primary myoblasts were washed with ice-cold PBS and RNA extracted using Trizol (Thermo Fisher Scientific). cDNA synthesis was performed using 1 μg of RNA, DNase I amplification grade (18068-015; Thermo Fisher Scientific) and Superscript III (18080-400; Thermo Fisher Scientific) according to manufacturer's instructions. Changes in gene expression were analyzed by quantitative RT-PCR (qRT-PCR) using Fast SYBR-Green master mix (Thermo Fisher Scientific) on the ABI StepOne Plus Sequence Detection System (Thermo Fisher Scientific) using the comparative C_t method (94) using *Ef1*α as control. The primers are listed in Supplemental Table S5.

ChIP assays

Three independent biologic replicates of proliferating and differentiating (24 h) primary myoblasts were cross-linked with 1% formaldehyde and incubated for 10 min at room temperature on an orbital shaker. To inactivate the formaldehyde, 1 ml of 1 M glycine was added and cells were incubated for 5 min on an orbital shaker at room temperature. Cells were washed 3 times with 10 ml of ice-cold PBS supplemented with cOmplete Protease Inhibitor (Roche, Basel, Switzerland). Cross-linked myoblasts were resuspended in 1 ml of ice-cold PBS supplemented with Complete Protease Inhibitor. The cell suspension was centrifuged for 5 min at 5000 *g* at 4°C. The PBS was removed and the cell pellet was resuspended in 200 μl of ice-cold SDS lysis buffer (50 mM Tris pH 8; 10 mM EDTA, 1% SDS) for 10 min. Proliferating myoblasts were sonicated 3 times for 5 min, 30 s by 30 s at mild intensity for myoblasts and 5 times for nascent myotubes using a Bioruptor UCD-200 (Diagenode, Denville, NJ, USA). The samples were diluted to a final volume of 1 ml in ChIP buffer (16 mM Tris pH 8.1; 1.2 mM EDTA; 0.01% SDS; 1.1% Triton ×100; 167 mM NaCl). ChIP was performed using a rabbit anti-MTF1 and a rabbit IgG antibodies. Samples were incubated for 2 h at 4°C in a rotating platform and subsequently, 80 μl of Magna ChIP protein A + G Magnetic Beads (MilliporeSigma) were added to each sample and incubated overnight in a rotating platform at 4°C. The samples were then placed in a magnetic rack and sequentially washed using 1 ml each of the wash buffer sequence A-D (buffer A: 20 mM Tris pH 8.1, 2 mM EDTA, 0.1% SDS, 1% Triton X-100, 167 NaCl, buffer B: 20 mM Tris pH 8.1, 2 mM EDTA, 0.1% SDS, 1% Triton X-100, 500 NaCl; buffer C: 10 mM Tris pH 8.1, 1 mM EDTA, 1% NP40, 1% sodium deoxicholate, 0.25 M $LiCl_2$; buffer D: 10 mM Tris pH 8.1, 1 mM EDTA). Immune complexes were eluted in 100 μl of buffer containing 0.1 M $NaHCO_3$, 1% SDS, 1 μg/μl proteinase K. Samples were then reverse cross-linked by adding 20 μl of 5 M NaCl and incubating overnight at 65°C. The reverse cross-linked DNA was purified using the ChIP DNA clean concentrator, following the manufacturer's instructions (Zymo Research, Irvine, CA, USA). The DNA was stored at −80°C until further analysis by semiquantitative real-time PCR (qPCR) or library preparation for ChIP-Seq. The MTF1 antibody used for ChIP was validated by Western blot using the recombinant purified mouse MTF1 protein and proved to be specific as shown by the KD of MTF1 using shRNA and CRIPSR/Cas9. Furthermore, we tested the binding of MTF1 to the promoter of Metallothionein 1 (*Mt1*), its classic target gene, which was enhanced by the addition of Cu to the medium (see below).

ChIP-seq

Library construction

Libraries of ChIP-enriched DNA were prepared from 2 biologic replicates following the Illumina strategy. Samples were end-repaired, A-tailed, and adaptor-ligated using barcoded inline adaptors according to the manufacturer's instructions (Illumina, San Diego, CA, USA). DNA was purified over a Zymo Research PCR purification column between each enzymatic reaction. DNA was PCR amplified with Kapa HiFi polymerase using 16 cycles of PCR. Each library was size-selected for 200–300 bp fragments on a 1.5% agarose gel and the library concentrations were determined using a QuBit 3.0 Fluorometer (Thermo Fisher Scientific). Libraries were sequenced on an Illumina HiSeq2000 using single-end 50 bp sequencing at the University of Massachusetts Medical School (Worcester, MA, USA) Deep Sequencing Core Facility.

Data analysis

Single-end Fastq reads were split by barcode adapter sequences and adapter sequences were removed using the Fastx toolkit. Reads were mapped to the mm10 genome using bowtie, allowing up to 3 mismatches. Aligned reads were processed using Hypergeometric Optimization of Motif EnRichment (HOMER) (95). University of California Santa Cruz (UCSC) UCSC genome browser tracks were generated using the "makeUCSCfile" command. Mapped reads were aligned over all annotated mm10 transcriptional start sites (TSSs) using the "annotatePeaks" command, generating 20 bp bins and summing the reads within each window. After anchoring mapped reads over reference TSSs, aggregation plots were generated by averaging data obtained from 2 biologic replicates. Peaks were called individually from replicate data sets using the "findPeaks" command and then overlapping peaks were identified using the "mergePeaks" command. For peak calling, a false discovery rate of 0.001 was used as a threshold. Motifs were identified using the "findMotifs" command. Analysis of data from GSE24852 (96) was performed similarly. Data were downloaded from GSE24852 and converted to Fastq files using SRAtoolkit Fastq-dump and mapped reads were converted to mm10. Aligned reads were processed in HOMER (95), as previously described.

Gene ontology term identification

Gene ontology (GO) term analysis was performed on metascape (*http://metascape.org*) (97).

Sequential ChIP

Primary myoblasts were lysed using the SimpleChIP Plus Sonication Chromatin IP Kit (Cell Signaling Technology), following the manufacturer's instructions. Briefly, after incubating the samples with MTF1 antibody and collecting immunoprecipitated material with magnetic beads, the samples were incubated with an equal volume of 10 mM DTT for 30 min at 37°C (98–100). The supernatant was used for the second immunoprecipitation (IP) by adding a rabbit anti-MYOD antibody and incubating the samples similarly to the first IP. IgG substituted for the MTF1 and MYOD antibodies served as a negative control.

Western blot analysis

Proliferating and differentiating primary myoblasts were washed with PBS and solubilized with RIPA buffer (10 mM PIPES, pH 7.4, 150 mM NaCl, 2 mM EDTA, 1% Triton X-100, 0.5% sodium deoxycholate, and 10% glycerol) containing cOmplete Protease Inhibitor. Protein was quantified by the Bradford method (101). Samples (20 μg) were prepared for SDS-PAGE by boiling in Laemmli buffer. The resolved proteins were electrotransferred to PVDF membranes (Bio-Rad, Hercules, CA, USA). The proteins of interest were detected with the specific polyclonal or monoclonal antibodies. Then the membranes were incubated for 2 h at room temperature with the species-appropriate peroxidase-conjugated antibodies (Thermo Fisher Scientific). Chemiluminescent detection was performed with ECL Plus (GE Healthcare, Chicago, IL, USA). Experiments were performed using samples from 3 independent biologic experiments. The quantification of Western blots was performed with ImageJ and reflect the relative amounts of MTF1 as the ratio of each protein band relative to the lane's loading control. Uncropped membranes for all the Western blots presented in this work are shown in Supplemental Figs. S7–S13.

Immunoprecipitation

Cells were washed 3 times with ice-cold PBS and resuspended in IP lysis buffer (50 mM Tris-HCl, pH 7.5, 150 mM NaCl, 1% Nonidet P-40, 0.5% sodium deoxycholate, and cOmplete protease inhibitor). Cell extracts were incubated with the anti-MTF1 primary antibody at 4°C for 2 h, followed by an overnight incubation with PureProteome Protein A/G mix magnetic beads (MilliporeSigma). Samples were washed as indicated by the manufacturer, and immunoprecipitated proteins were eluted in freshly prepared IP-elution buffer (10% glycerol, 50 mM Tris-HCl, pH 6.8, and 1 M NaCl) at room temperature for 1 h (41). Samples were analyzed by SDS-PAGE and Western blot.

Subcellular fractionation of primary myoblasts and metal content analysis

Three independent biologic replicates of proliferating and differentiating (24 h) primary myoblasts were fractionated using the Rapid, Efficient, and Practical nuclear and cytoplasmic separation method (102). Briefly, cells were washed with ice-cold PBS, scraped, and transferred to a 1.5-ml microcentrifuge tube. Samples were centrifuged for 10 s at 13,000 *g* and the supernatant was discarded. The samples were resuspended in 500 μl of ice-cold PBS containing 0.1% NP40 (MilliporeSigma) and 100 μl of the cell suspension were collected as the whole cell fraction. The remaining 400 μl were used to obtain nuclear and cytosolic fractions by disrupting the cells by pipetting using a 1-ml pipette tip. Cell suspension was centrifuged for another 10 s and the supernatant was collected as the cytosolic fraction. The nuclear pellet was then washed twice in 1 ml of ice-cold PBS containing 0.1% NP40 and once again centrifuged for additional 10 s. The supernatant was removed and pellet was resuspended in 100 μl of PBS. Nuclear integrity was verified by light microscopy. All samples were sonicated at medium intensity for 5 min in 30 s on 30 s off cycles. Protein was quantified by the Bradford method (101). Purity of the fractions was evaluated by Western blot.

The comparative analysis of Cu concentrations from each sample was carried out using an atomic absorbance spectroscopy (AAS) equipped with a graphite furnace (AAnalyst 800; PerkinElmer, Waltham, MA, USA). A known mass of sample was acid digested in concentrated HNO_3, using a single-stage digestion method (103, 104). All measurements were performed in triplicate, resulting in a limit of detection for Cu of 15, and 10 ppb for Zn calculated as 3σ and were performed as previously described (42, 105). Analytical grade standards for Cu and Zn were used and diluted in 18 MΩ purified water. Cu and Zn content on each sample was normalized to the initial mass of protein.

Expression and purification of recombinant MTF1

Plasmids coding for MTF1 WT and the MBS mutant proteins were transformed into Stbl3 cells for propagation and transformed into BL21 DE3 bacteria for expression. Recombinant protein expression was performed according to an auto-inducing medium protocol (106). Purification of GST-tagged WT and mutated MTF1 recombinant proteins was carried out using Glutathione Agarose resin as described by the manufacturer (Pierce, Rockford, IL, USA). Purified proteins were stored at −20°C in buffer containing 10% glycerol, 100 mM Tris, pH 8, and 150 mM NaCl. Protein concentrations were determined by the Bradford assay (101). Molar protein concentrations were estimated using MW 81,000 Da for both MTF1 proteins. In order to eliminate any bound metal, all purified proteins were treated with metal chelators as previously described (107–110). Briefly, the proteins were incubated for 45 min at room temperature with 0.5 mM EDTA and 0.5 mM tetrathiomolybdate. Chelators were removed by buffer exchange using either 50 kDa cutoff Centricons (MilliporeSigma). The final purity of all protein preparations was ≥95%, as verified by SDS-PAGE followed by Coomassie Brilliant Blue staining (Thermo Fisher Scientific) and Western blot.

Cu loading to MTF1 and metal binding analyses

Cu^+ loading was performed by incubating each apo-protein (10 μM) in the presence of 10 M excess of $CuSO_4$, 25 mM Hepes (pH 8.0), 150 mM NaCl, and 10 mM ascorbate for 10 min at room temperature with gentle agitation, as previously described by Padilla-Benavides *et al.* (110). The unbound Cu was removed by washing in 50 kDa cutoff Centricons. Levels of Cu bound were verified by AAS, Varian. Briefly, before determinations, sample aliquots were mineralized with 35% HNO_3 (trace metal grade) for 1 h at 80°C, and digestions were concluded by making the reaction 3% H_2O_2. Metals bound to WT and mutant MTF1 were measured in triplicate using a method similar to the subcellular fractionation of primary myoblasts (*vide supra*).

Statistical analyses

In all cases, the data represent the mean of 3 independent biologic replicates ± SD; 1-way ANOVA, followed by Bonferroni multiple

comparison tests using Kaleidagraph v.4.5 (Synergy Software, Reading, PA, USA).

Data availability

Genomic data sets have been deposited within Gene Expression Omnibus (GEO) (accession no. GSE116331).

RESULTS

MTF1 is up-regulated during differentiation of primary myoblasts

MTF1 is a metal binding TF that is primarily involved in the control of metal and redox homeostasis (56, 58, 60, 66, 68, 69, 82, 83, 85, 111–115). There is also evidence to suggest that MTF1 is involved in developmental processes (57, 61, 63, 116). We hypothesized that MTF1 may play an active role in the determination of the myogenic lineage. To test this hypothesis, we analyzed both the expression and localization of MTF1 in primary myoblasts derived from mouse satellite cells. Western blot analyses showed minimal expression of the MTF1 protein in proliferating primary myoblasts (**Fig. 1*A, B***). However, MTF1 protein expression was up-regulated when differentiation was induced, as shown by the expression of myogenic markers (Fig. 1*A, B*). Confocal microscopy imaging of MTF1 is consistent with Western blot analyses (Fig. 1*C*). Proliferating primary myoblasts have low levels of MTF1 in a punctate cytosolic distribution. Upon induction of MYOD, MTF1 expression increased and was primarily localized to the nucleus. At 48 and 72 h after initiation of differentiation, the distribution of MTF1 was primarily nuclear, although there was an increase in the cytosolic puncta that is consistent with its role in metal sensing. These data indicate that differentiation induces MTF1 expression and nuclear localization.

Mtf1 is required for myoblast differentiation

To determine the physiologic role of MTF1, we used viral vectors encoding shRNA to KD *Mtf1*, and the CRISPR/Cas9 system to generate *Mtf1*-deficient primary myoblasts. Two lentiviral constructs that encode for shRNAs against *Mtf1* mRNA were used to knock down the endogenous protein in proliferating and differentiating primary myoblasts. Myoblasts transduced with a lentivirus-encoded nonspecific *scr* shRNA were used as negative controls. The infected cells were selected with puromycin and levels of *Mtf1* were examined by Western blot analysis

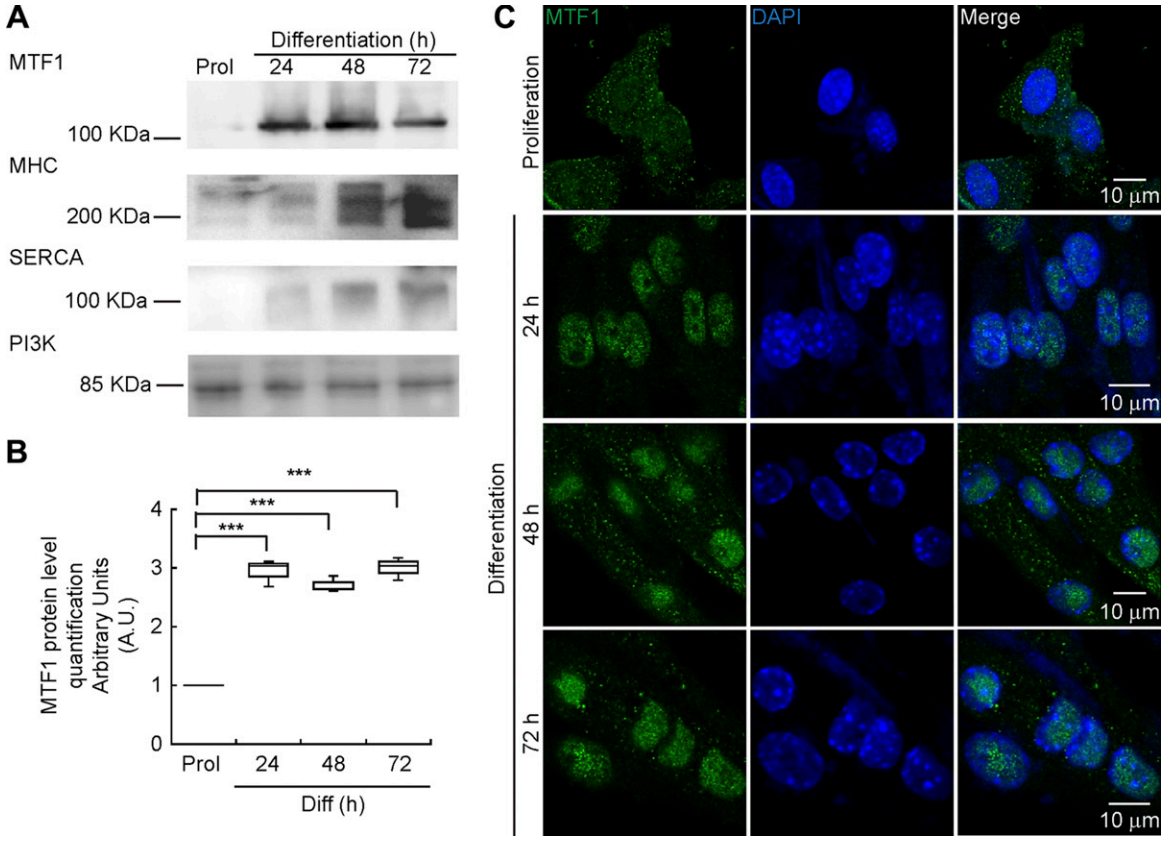

Figure 1. MTF1 is induced upon induction of differentiation of primary myoblasts. *A*) Representative Western blot of MTF1 expression; the MYOD markers examined were myosin heavy chain (MHC) and the SERCA from proliferating and differentiating primary myoblasts at 24, 48, and 72 h. PI3K was used as loading control. *B*) Densitometric quantification of MTF1 bands in proliferating and differentiating (24, 48, and 72 h) primary myoblasts. ***$P < 0.001$. *C*) Representative confocal microscopy images of proliferating and differentiating primary myoblasts at 24, 48, and 72 h for MTF1 (green), and DAPI (blue). Images depicted are representative of ≥3 independent biologic experiments.

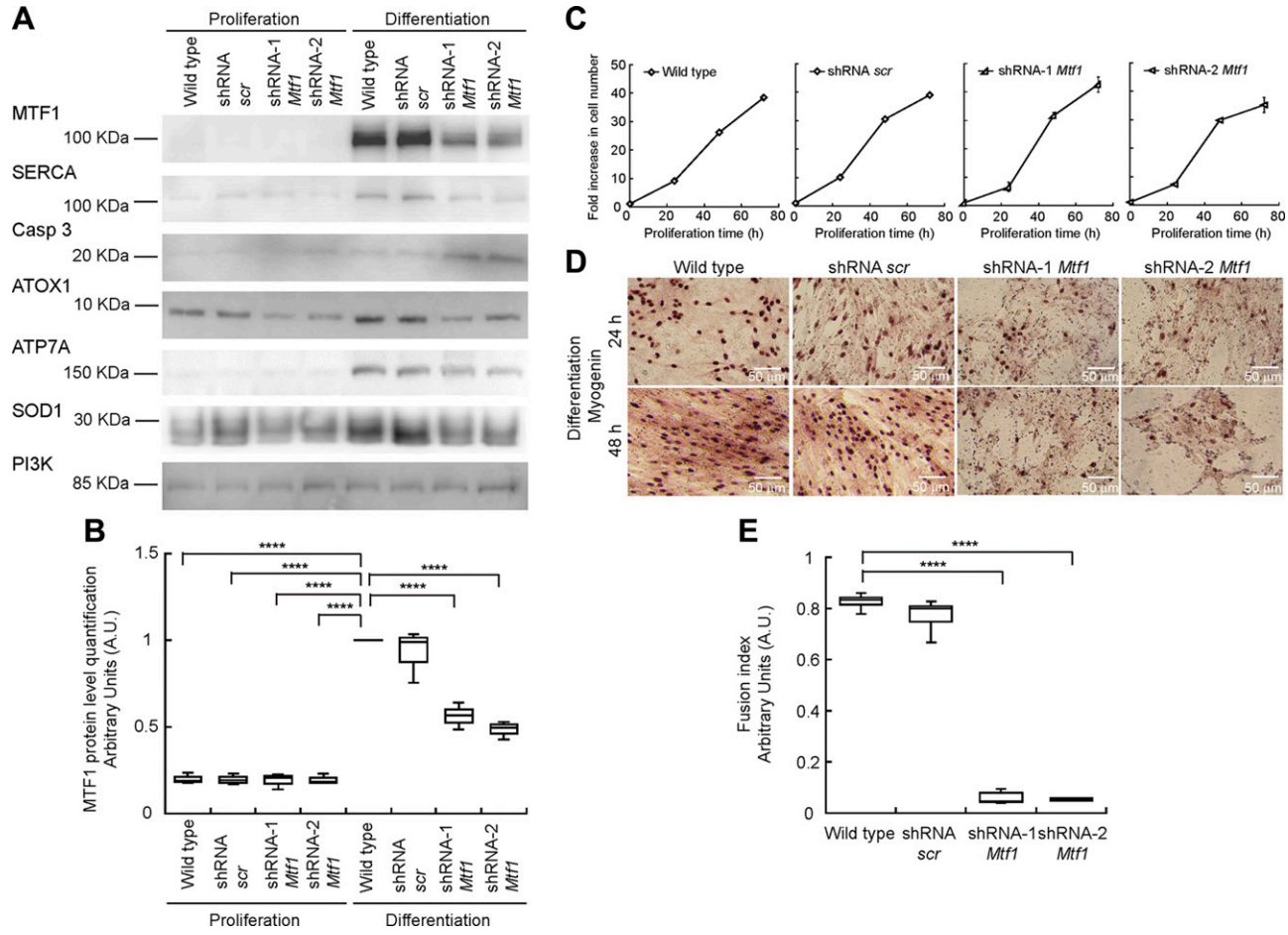

Figure 2. Partial depletion of MTF1 using shRNA impairs myogenesis and partially leads to death of differentiating myoblasts. *A*) Representative Western blot of primary myoblasts and myoblasts transduced with either *scr* shRNA or 2 different shRNAs against *Mtf1* (1, 2) during proliferation and 24 h after inducing differentiation. SERCA levels were monitored as a differentiation marker; cleaved Caspase-3 as marker of cell death. The analyzed cuproproteins were the Cu^{+}-chaperone ATOX1, the Cu^{+}-transporter ATP7A, and SOD1. GAPDH was used as a loading control. *B*) Densitometric quantification of MTF1 bands in proliferating and differentiating (24, 48, and 72 h) primary myoblasts in *A*. *C*) Proliferation curves comparing WT, *scr* control, and *Mtf1* (shRNA 1 and 2) partially depleted primary myoblasts. No significant differences were found between the 4 strains. Data represent the mean of 3 independent experiments ± SD. *D*) Representative light micrographs of differentiating myoblasts immunostained for myogenin at 24 and 48 h. *E*) Calculated fusion index for *Mtf1*-sgRNA–transduced myoblasts. Box plots represent the distribution of the data obtained from 3 independent biologic experiments ± SD. ****$P \leq 0.0001$.

(**Fig. 2**). Differentiating myoblasts transduced with *Mtf1* shRNA showed a significant decrease in the expression of MTF1 protein compared to WT and *scr* shRNA controls (Fig. 2*A, B*). *Mtf1* KD cells had similar growth kinetics compared to WT cells, suggesting that proliferating primary myoblasts can tolerate MTF1 KD (Fig. 2*C*). These results suggest that the primary role of MTF1 in proliferating myoblasts is maintenance of metal homeostasis as opposed to regulation of the cell cycle. To determine whether partial loss of MTF1 impaired myogenesis, *Mtf1* shRNA–transduced primary myoblasts were induced to differentiate. Western blot analyses for the differentiation marker sarco/endoplasmic reticulum Ca^{2+}-ATPase (SERCA) showed decreased levels in myoblasts partially depleted of MTF1 (Fig. 2*A*). IHC analyses where differentiating myoblasts were stained with an antimyogenin antibody confirmed that *Mtf1* KD cells fail to differentiate because they had a decreased incidence of myogenin-positive nuclei compared to WT and *scr* shRNA–transduced myoblasts (Fig. 2*D*). Detachment of *Mtf1* KD cells was observed upon induction of differentiation (Fig. 2*D*), and these cells had shown a significantly lower fusion index than WT cells (Fig. 2*E*). Western blot analyses showed an increased expression and activation of the apoptotic marker Caspase-3 in differentiating myoblasts partially depleted of *Mtf1* (Fig. 2*A*). Together these data demonstrated a requirement for MTF1 during the differentiation of primary myoblasts derived from mouse satellite cells.

It is well established that MTF1 contributes to the expression of several metalloproteins. Further, our group has shown that the Cu transporters ATP7A and copper transporter 1 (CTR1) are induced during myogenesis (35). Therefore, we asked if *Mtf1* KD would have an impact on the expression of these and other representative cuproproteins, which are known to maintain the cytoplasmic and mitochondrial Cu levels. Representative Western blot analyses showed that the chaperone ATOX1, the Cu^{+}-transporter ATP7A, and SOD1 were induced during

myogenesis (Fig. 2*A*). Consistent with a role in the regulation of these cuproproteins, *Mtf1* KD partially blocked the differentiation-dependent induction of these proteins observed in control cells. These data suggest that the role of MTF1 in myogenesis may be partially due to its effect in the proteins that regulate Cu homeostasis. However, these data do not exclude the possibility that MTF1 may contribute to the transcriptional regulation of additional lineage-specific genes.

The biologic relevance of MTF1 during myogenesis was confirmed by targeting the *Mtf1* locus with CRISPR/Cas9. Western blot analyses of differentiating primary myoblasts at 24 h showed over 90% reduction in MTF1 protein and gene levels (Supplemental Fig. S1). Consistent with our observations using shRNA (Fig. 2), MTF1 loss correlated with a failure to differentiate as shown by a decrease in protein levels and gene expression of myogenic markers SERCA, myogenin, and muscle-specific creatine kinase (Supplemental Fig. S1*A–C*). *Mtf1*-deficient cells proliferated normally and showed no visible phenotype during initial passages (Supplemental Fig. S1*D*); however, extended culture (5 passages) of these cells resulted in increased apoptosis relative to control cells (unpublished results), suggesting that the MTF1-deficient cells are sensitive to extended passage in tissue culture. IHC analysis showed that *Mtf1*-deficient cells detached from the plates at 24 h after induction of myogenesis and presented a lower fusion index than control cells (Supplemental Fig. S1*E, F*), which correlates with increased cleaved Caspase-3, as compared to WT and empty vector sgRNA myoblasts (Supplemental Fig. S1*A*). Overall, these results show that MTF1 plays an essential functional role in myogenic gene regulation and contributes to cell survival upon initiation of MYOD.

MTF1 expression is enhanced by Cu ions

In order to induce myogenesis in cultured myoblasts, growth factors are depleted by serum starvation and insulin is added (88, 117). Depletion of insulin from the differentiation medium partially prevents MYOD, a phenotype that we have shown can be rescued by the addition of nontoxic (30 μM) concentrations of $CuSO_4$ (35). Moreover, depletion of Cu from the culture medium inhibits differentiation, which suggests that Cu plays a role in differentiation (35). However, the molecular mechanisms by which Cu affects differentiation are largely unknown. To probe for links between Cu ions and MTF1, we cultured primary myoblasts under different concentrations of Cu and determined the expression levels of MTF1 through Western blot and qRT-PCR. **Figure 3** shows that MTF1 expression was significantly increased in cells grown in medium depleted of insulin and supplemented with 30 μM $CuSO_4$ compared to those grown in basal differentiation medium containing insulin. By contrast, Cu chelation with TEPA resulted in a significant decrease in MTF1 expression. Addition of $CuSO_4$ at a concentration equal to that of TEPA restored the expression levels of MTF1 to those observed in cells differentiated under normal insulin conditions. Insulin depletion had a similar effect on MTF1 expression as TEPA treatment. These data indicate a role for Cu ions in MTF1 induction during myogenesis. Importantly, we detected an increase in the expression of the differentiation marker SERCA when cells were treated with Cu, which was abolished when cells were depleted of Cu by addition of TEPA (Fig. 3*A*). These data are consistent with our previous studies in which the expression of myogenin and other differentiation markers was enhanced by Cu supplementation (35).

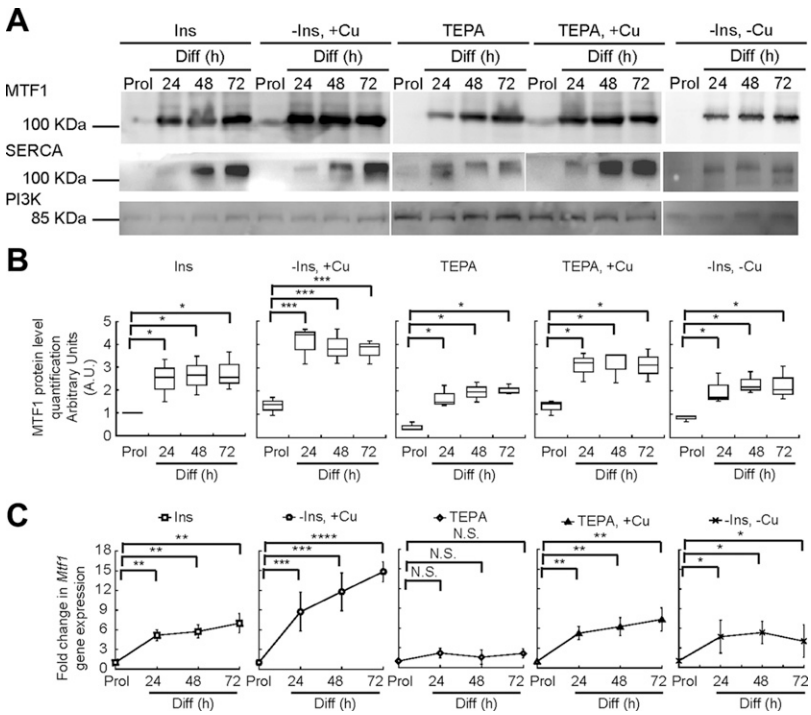

Figure 3. Cu enhances the expression of MTF1 in differentiating myoblasts. *A*) Representative Western blots of MTF1 and SERCA in proliferating and differentiating myoblasts differentiated in the presence or absence of insulin, Cu, and TEPA as indicated. PI3K was used as loading control. *B*) Densitometric quantification of MTF1 bands in proliferating and differentiating (24, 48, and 72 h) primary myoblasts. *C*) Steady-state mRNA levels of *Mtf1* determined by qRT-PCR from proliferating and differentiating primary myoblasts cultured in the same conditions described in *A*. Box plots represent the distribution of the data obtained from 3 independent biologic experiments ± SD. $^*P < 0.05$, $^{**}P < 0.01$, $^{***}P < 0.001$.

MTF1 binds to the promoters of myogenic genes in differentiating myoblasts

Our data thus far indicate that MTF1 is required for myogenesis in addition to its role in maintaining metal homeostasis. We hypothesized that Cu enhances the transcriptional activity of MTF1 and that MTF1 globally regulates the expression of genes required for skeletal muscle differentiation. To test this, we performed ChIP-Seq to identify MTF1 binding sites on chromatin in primary myoblasts differentiated for 24 h under normal insulin conditions. Genome-wide analyses showed that in the presence of insulin, MTF1 localized largely to promoters around TSSs (**Fig. 4*A***). MTF1 binding to TSSs was enhanced by the addition of $CuSO_4$ to the culture medium. Cells grown in culture medium depleted of insulin had decreased MTF1 binding that was similar to the input controls (Fig. 4*A*).

Next, we called peaks for MTF1 in differentiating myoblasts. We found 1399 MTF1 peaks for myoblasts differentiated under normal insulin conditions, 2713 for cells differentiated in the presence of Cu, and only 553 peaks for the cells depleted of insulin. Strikingly, 993 peaks were shared between the cells differentiated with insulin

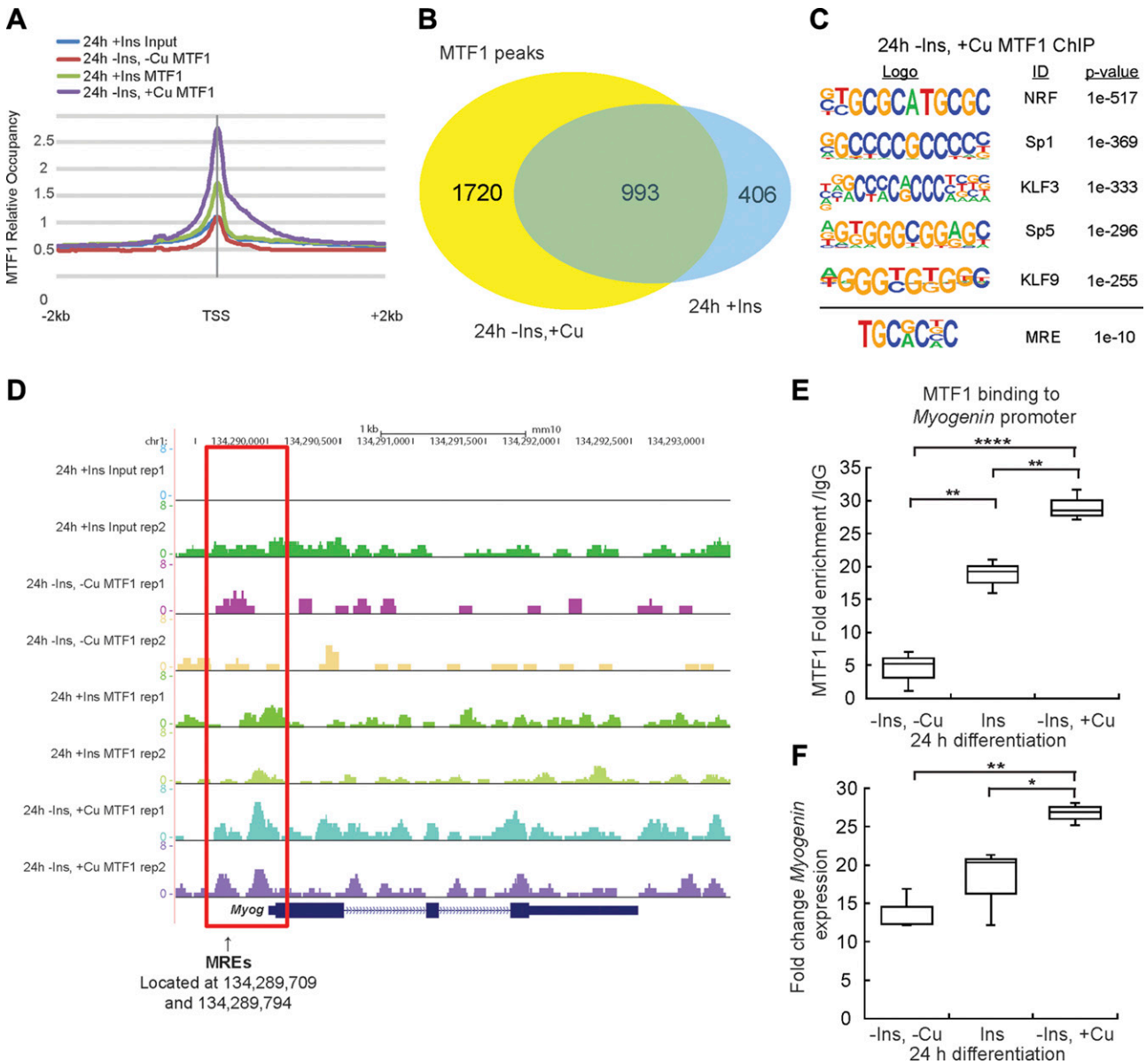

Figure 4. MTF1 binding in differentiating primary myoblasts. *A*) Aggregation plots of MTF1 ChIP-Seq data showing occupancy over annotated TSSs. *B*) Overlap of ChIP-Seq peaks of MTF1 across the genome observed in differentiating cells in the presence of insulin or Cu. *C*) Novel consensus DNA-binding motifs identified within MTF1 peaks. Shown are MRE and the top 5 most significant motifs enriched, including the DNA logo, its corresponding TF, and its *P* value. *D*) Genome browser tracks of replicate ChIP-Seq experiments examining MTF1 binding to the *Myogenin* promoter in differentiating myoblasts (24 h) under different culture conditions. *E*) ChIP-qPCR validation for MTF1 binding to the *Myogenin* promoter. *F*) Steady-state mRNA levels of *Myogenin* in differentiating primary myoblasts cultured in the same conditions as indicated in *E*. Box plots represent the distribution of the data obtained from 3 independent biologic experiments. $^{**}P < 0.01$, $^{****}P \leq 0.0001$.

and the cells differentiated with Cu (Fig. 4*B* and Supplemental Table S1). GO analyses showed that MTF1 binds to diverse categories of genes associated with muscle development, function, and, as expected, ion homeostasis (Supplemental Fig. S2 and Supplemental Table S2).

MTF1 is known to preferentially bind the MRE consensus sequence, -TGCRCNC- (70–72). As expected, ChIP-Seq analyses showed MTF1 enriched binding to this motif (Fig. 4*C* and Supplemental Table S1). In the presence of insulin or $CuSO_4$, 32% and 38% of the MTF1 peaks contained a consensus MRE sequence, respectively. This result suggests direct binding by MTF1 to MREs as 1 mechanism of MTF1-mediated gene activation but also suggests that MTF1 is interacting with chromatin indirectly through other TF binding sites. We performed a *de novo* motif search on the Cu-specific MTF1 peaks to identify additional binding motifs for MTF1. The regions under MTF1 peaks had high GC contents, and the top 5 motifs are shown (Fig. 4*C* and Supplemental Table S1). The most significant of these motifs matches to the binding motif for the TF nuclear respiratory factor. Nuclear respiratory factors 1 and 2 play a role in the expression of nuclear and mitochondrial genes involved in oxidative phosphorylation, electron transport complexes I–V, and mitochondrial (mt)DNA transcription and replication (118, 119), all processes important in skeletal muscle function. The second most significant motif matches the binding site of Sp1, a TF that has been shown to regulate muscle gene expression in concert with MyoD (120). The next most significant motifs correspond to Krüppel-like factor (KLF3), specificity protein 5 (SP5), and KLF9, each of which has been linked to skeletal muscle differentiation or function (121–124). These data suggest that MTF1 may bind chromatin in conjunction with multiple diverse regulators to regulate gene expression during muscle differentiation.

We found the conserved MRE sequence for MTF1 binding at some myogenic genes, such as *Myogenin*, which encodes the classic transcriptional activator that is expressed upon initiation of myogenesis and is essential for the transcription of muscle-specific genes (40, 46, 125, 126). Bioinformatic analyses revealed that 2 potential MREs, 5′-TGCACAG-3′ and 5′-TGCACCC-3′, are located at 300 and 400 base pairs upstream, respectively, of the *Myogenin* TSS. Therefore, we hypothesized that MTF1 may bind near the promoter of *Myogenin*. To test this, we assessed our ChIP-Seq data over the *Myogenin* promoter and found that MTF1 binding was enriched by Cu supplementation (Fig. 4*D*). We detected that MTF1 enrichment at the 2 sites in the *Myogenin* promoter was different in myoblasts treated with insulin and Cu. Interestingly, MTF1 binding to the MRE was higher in myoblasts cultured with Cu than control cells, suggesting that Cu induces higher binding to this promoter than insulin alone, which is potentially related with increased expression of the gene. In addition to enrichment at the promoter-proximal MREs, we observed above background enrichment of MTF1 within the *Myogenin* gene body, raising the possibility that either additional MTF1 binding sites were found within the *Myogenin* gene or MTF1 interacts with additional regulatory proteins bound within the gene body. The binding of MTF1 to the *Myogenin* promoter was validated by ChIP-qPCR, which showed a significant increase in MTF1 binding under normal differentiation conditions as well as when the myoblasts were differentiated in medium supplemented with 30 μM $CuSO_4$ (Fig. 4*E*). Similarly, *Myogenin* expression was robustly induced under both conditions (Fig. 4*F*), demonstrating that Cu supplementation can promote both MTF1 binding and *Myogenin* activation.

Binding of MTF1 was evaluated at additional myogenic genes by ChIP-Seq and ChIP-qPCR. There is enhanced binding of MTF1 to the promoter of A disintegrin and metalloproteinase 9, a membrane anchored cell surface adhesion protein that mediates cell-cell and cell-matrix interactions and muscle development (Supplemental Fig. S3*A, B*) (127). MTF1 was also found at the promoters of additional myogenic genes, such as *MyoD, Integrin 7a*, *Skeletal actin*, *Myf5*, and *Cadherin 15* (Supplemental Table S2). To validate our ChIP-Seq analyses, we evaluated MTF1 binding to its classic target promoter, *Mt1*. ChIP-qPCR data showed that MTF1 binding to the *Mt1* promoter is enhanced upon addition of 30 μM $CuSO_4$ to the culture medium of primary myoblasts, as expected (Supplemental Fig. S3*C, D*). As a negative control, no binding to the *Pax7* promoter was observed (Supplemental Fig. S4).

MTF1 interacts with MyoD and binds a subset of MyoD-bound loci

Interestingly, the classic DNA-binding motif (E-box) of MYOD was included among the TF binding sites found within MTF1 peaks, suggesting a potential novel interaction at promoter regions for both TFs (Supplemental Table S1, line 33). MYOD and MyoD-related factors initiate the regulation of skeletal muscle gene expression through direct binding of the myogenic gene promoters during differentiation (120, 128). We hypothesized that MTF1 may interact with MYOD, forming a complex that binds the promoters of myogenic genes that MYOD regulates. We first investigated whether MTF1 and MYOD physically interact in primary myoblasts differentiated for 24 h. IP assays using an anti-MTF1 antibody revealed that MTF1 coprecipitated with MYOD upon initiation of myogenesis in both the presence and absence of Cu (**Fig. 5*A***). To further characterize the functional relationship between MTF1 and MYOD, we compared the ChIP-Seq data sets for MYOD in differentiated primary myoblasts (10 and 48 h) from Soleimani *et al.* (96), with our MTF1 ChIP-Seq data. We found 714 peaks shared between MYOD and MTF1 when myoblasts were differentiated in the presence of Cu, which represents over 25% of the total number of MTF1 peaks (Fig. 5*B*). GO term analyses of these peaks showed MyoD and MTF1 bind to myogenic genes, but also metal ion transport and homeostasis genes (Supplemental Fig. S2 and Supplemental Table S3). *De novo* motif identification of overlapping MyoD and MTF1 peaks gives a similar outcome as the analysis of motifs under MTF1 peaks (Figs. 4*C* and 5*C*). Analysis of individual genes for MTF1 and MyoD binding showed increased peaks at the same promoter region of the *Myogenin* gene (Fig. 5*D*). This cobinding was confirmed by sequential

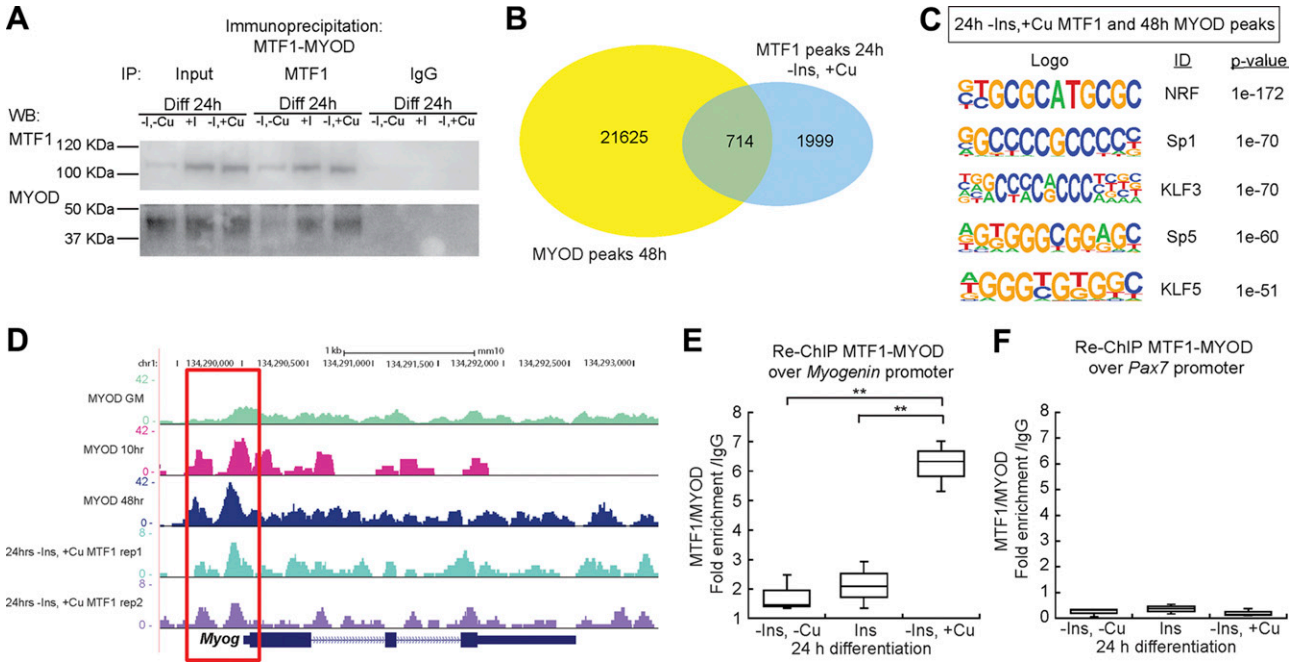

Figure 5. MTF1 interacts with MyoD at the promoter regions of myogenic genes. *A*) Representative Western blot of MTF1-MYOD IP using the rabbit anti-MTF1 antibody. Pulldown with IgG was used as a negative control. *B*) Overlap of MTF1 ChIP-Seq peaks from primary myoblasts differentiated with Cu MTF1 and MYOD peaks extracted from data sets published by Solemaini *et al.*, (96) (GSE24852). *C*) Consensus binding motifs identified for sequences bound by MTF1 and MYOD. Shown are the top 5 most significant motifs enriched, including the DNA logo, its corresponding TF, and its *P* value. *D*) Genome browser tracks of ChIP-Seq data comparing MTF1 occupancy at the myogenin locus in cells 24 h after differentiation with Cu (as shown in Fig. 4) and MYOD occupancy at the myogenin locus in proliferating growth medium (GM) cells or cells differentiated for 10 or 48 h. MYOD ChIP-Seq data was downloaded and analyzed from GSE24852 [Soleimani *et al.* (96)]. *E, F*) Reciprocal ChIP–qPCR for MTF1-MYOD cobinding to the *Myogenin* promoter (*E*) and to the *Pax7* promoter (*F*) as a negative control. Box plots represent the distribution of the data obtained from 3 independent biologic experiments. $^{**}P < 0.01$.

reciprocal ChIP analyses of MyoD and MTF1, which indicated that both TFs co-occupy the *Myogenin* promoter in myoblasts (Fig. 5*E*). We did not detect cobinding of the MTF1-MyoD complex to the *Pax7* promoter region (Fig. 5*F*), which further supports our conclusion that MTF1 regulates differentiation-specific gene expression. Together, these data suggest that MYOD and MTF1 form a stable complex on chromatin in differentiating primary myoblasts to regulate the transcription of a common set of myogenic target genes. However, even though we identified an interaction between MTF1-MYOD, this interaction likely does not occur at all sites on chromatin. Furthermore, given that these 2 TFs have divergent roles, we cannot overrule the possibility that other factors mediate interaction between MTF1 and MYOD at certain promoters, or further posttranscriptional modifications that may occur to promote or prevent interaction at some locations. We emphasize that the data indicate that only a subset of myogenic genes are bound by both MYOD and MTF1, suggesting that MTF1 acts through multiple regulatory mechanisms.

MTF1 binds Cu, which may play a role in its nuclear translocation and enhanced binding to myogenic promoters

We recently reported that differentiating myoblasts accumulate Cu, which is consistent with the inherent requirement for this metal during myogenesis (35). Consistent with this hypothesis, AAS analyses showed that the increase in Cu levels observed in differentiating myoblasts is prevented upon Cu chelation (**Fig. 6*A***). Subcellular fractionation of proliferating and differentiating myoblasts showed that Cu is mobilized to the nucleus upon induction of myogenesis (Fig. 6*B*). Cells grown in the presence of Cu had higher levels of Cu in the nucleus than did control cells during proliferation. Lower levels of nuclear Cu were detected in myoblasts differentiated in the presence of TEPA (Fig. 6*B*). Cytosolic concentrations of Cu were higher than in the nucleus under all conditions tested (Fig. 6*C*). Purity of the fractions was determined by Western blot analysis of lysates from primary myoblasts differentiated with insulin; Pol II was used to identify the nuclear fraction and β-tubulin for the cytosolic fraction (Fig. 6*D*) (105).

We hypothesized that the potential of MTF1 to bind Cu may contribute to the nuclear translocation and enhanced activation of this TF. Interestingly, *Drosophila* MTF1 contains a carboxy-terminal cysteine-rich Cu^+-binding domain, distinct from its Zn finger domains that bind Zn ions, that is proposed to sense excess intracellular Cu and participate in the cellular heavy metal response (74, 86). Mammalian MTF1 has a similar putative Cu^+-binding domain at its C-terminal domain. To test for a similar function, we cloned, expressed, and purified WT murine recombinant MTF1 (**Fig. 7*A***). We first examined the Cu^+-binding properties of the purified protein by incubating it

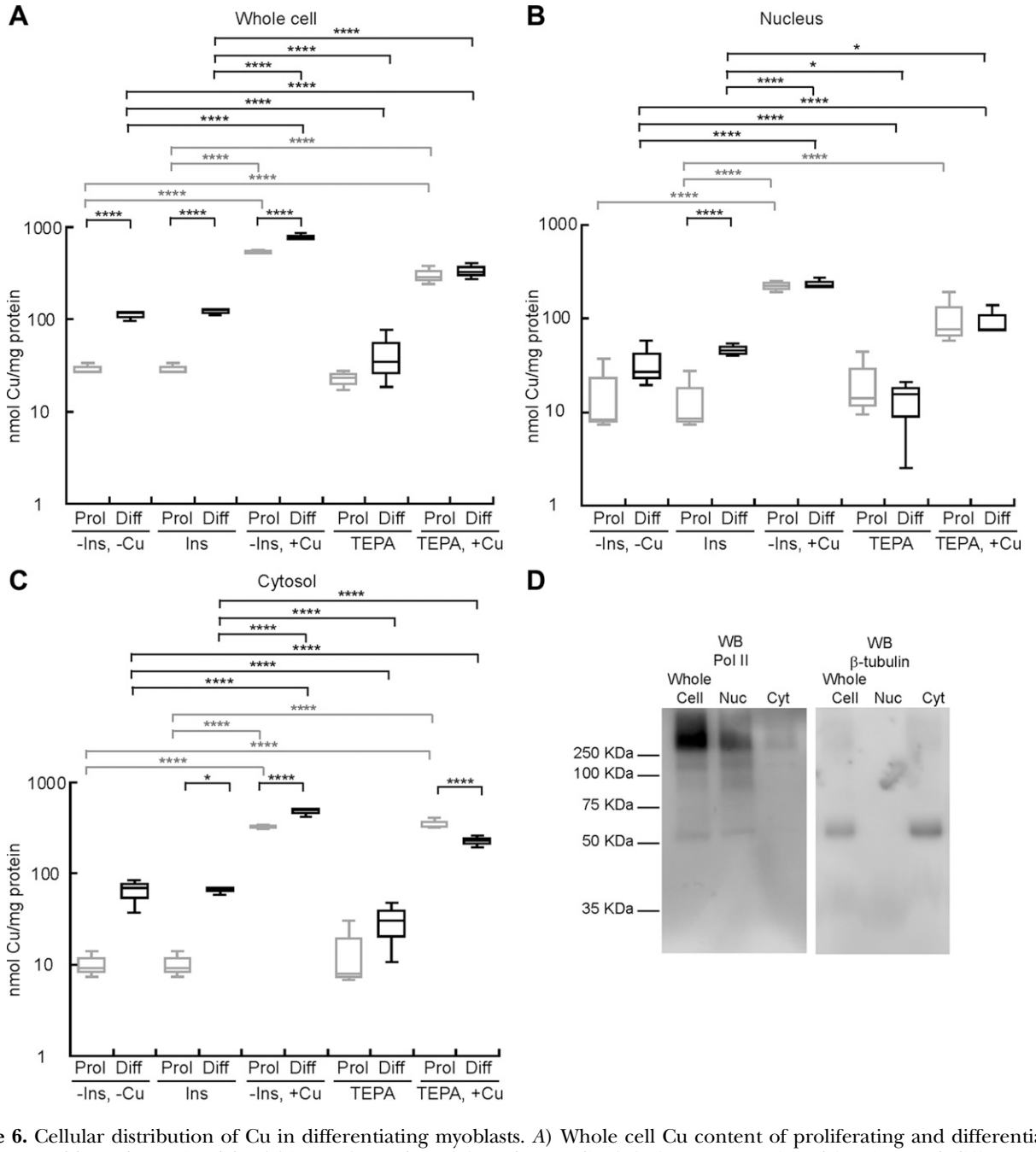

Figure 6. Cellular distribution of Cu in differentiating myoblasts. *A*) Whole cell Cu content of proliferating and differentiating primary myoblasts determined by AAS. *B, C*) Nuclear (*B*) and cytosolic (*C*) Cu content of proliferating and differentiating primary myoblasts cultured under different Cu conditions. Metal determination was performed by AAS. Box plots represent the distribution of the data obtained from 3 independent biologic experiments; $*P < 0.05$, $****P \leq 0.0001$. *D*) Representative Western blot showing the purity of the subcellular fractions. RNA polymerase II, and β-tubulin were used as controls to show the separation of nuclear and cytoplasmic fractions.

with excess Cu^+ in the presence of ascorbate as a reducing agent. Metal determinations by AAS revealed that Cu^+ interacts with MTF1 at a stoichiometry of 1.17 ± 0.06 Cu atoms per protein (Fig. 7*B*). To test whether Cu binds at the C-terminal cysteine-rich domain, we mutated the 4 key cysteine residues to alanines (MBS, Fig. 7*A*). These mutations strongly impaired binding of Cu^+ to MTF1 (Fig. 7*B*), implicating these amino acids in Cu^+ binding.

These data raise the possibility that MTF1 contributes, at least in part, to the translocation of Cu ions to the nucleus. To test this hypothesis, we took advantage of primary myoblasts partially depleted of *Mtf1* by shRNA (Fig. 2) and performed complementation experiments using a retroviral overexpression system to reintroduce *Mtf1* WT or MBS constructs to the cells (**Fig. 8*A***). First, we verified that both *Mtf1* constructs were expressed and whether they had an effect in myogenesis. Immunodetection analyses using an anti-Flag and anti-MTF1 antibodies show the expression of MTF WT and MBS in proliferating and differentiating primary myoblasts (Fig. 8*A*). Confocal microscopy analyses showed that both proteins efficiently translocated to the nuclei of myoblasts

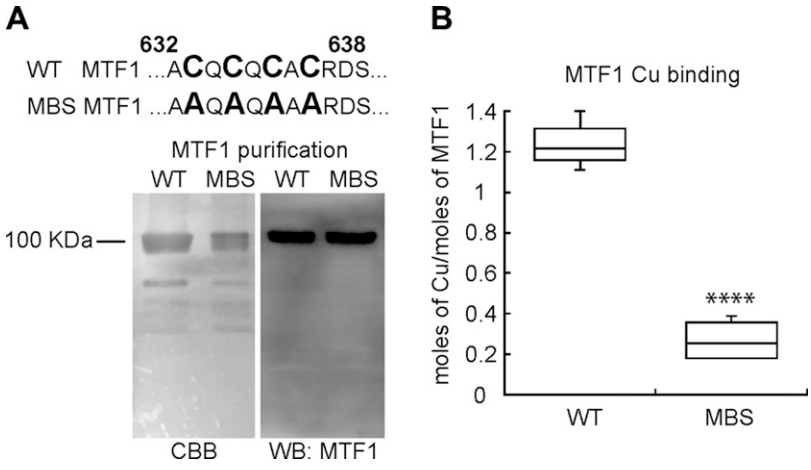

Figure 7. The tetra-cysteine cluster of MTF1 binds Cu *in vitro*. *A*) Upper panel depicts the sequence containing the tetra-cysteine cluster at the carboxy-terminal of the murine MTF1 that is required for transcriptional response to Zn and Cd (aa 632, 634, 636, and 638) (86). These residues were mutated to Alanine to assess Cu-binding capabilities of this putative metal-binding site (MBS). Lower panel shows a representative Coomassie Brilliant Blue–stained SDS/PAGE and a Western blot immunostained with anti-MTF1. *B*) Cu-binding stoichiometry of purified WT and MTF mutated at the MBS determined by AAS. Box plots represent the distribution of the data obtained from 3 independent biologic experiments. $^{****}P \leq 0.0001$.

undergoing differentiation (Fig. 8*B*), and were capable of restoring the differentiation phenotype, as shown by the expression of SERCA (Fig. 8*A*) and myogenin (Fig. 8*C*). However, myoblasts expressing the MTF1 MBS construct presented a differentiation delay compared to control cells (Fig. 8*C*), which was confirmed by a decreased fusion index (Fig. 8*D*). These results were recapitulated in differentiating primary myoblasts depleted of *Mtf1* by CRISPR/Cas9 expressing both constructs (Supplemental Fig. S5). Importantly, ChIP-qPCR analyses showed the exogenous MTF1 WT and MBS expressed in *Mtf1* KD myoblasts shRNA are able to bind to the *Myogenin* promoter in the presence of insulin but to a lower extent than in control cells (Fig. 8*E*). However, in the presence of Cu, an increased binding for both MTF1 constructs was observed at the *Myogenin* promoter, but only the binding of the WT protein was similar to control cells (Fig. 8*E*). In contrast, ChIP-qPCR analyses performed in differentiating *Mtf1* CRISPR/Cas9 myoblasts confirmed that the WT protein binds to the *Myogenin* promoter at levels equivalent to that observed in control cells, whereas the MTF1 MBS mutant is severely impaired for binding to this locus (Supplemental Fig. S5*E*). The greater inhibition of binding observed in the *Mtf1* CRISPR/Cas9 cells likely reflects the greater reduction of endogenous MTF1 protein in these cells compared to the reduction in the shRNA-treated cells.

We then evaluated whether MTF1 KD or the specific mutation of the tetra-nuclear cysteine cluster would impair the capability of the cells to accumulate and translocate Cu into the nucleus. First, we evaluated the whole cell levels of Cu in WT myoblasts, cells transduced with *scr* and *Mtf-1* and 2 shRNA, and KD cells recovered with exogenous WT or MBS MTF1 (Fig. 8*F*). Overall, *Mtf1* KD cells exhibited a significant decrease in the total levels of Cu upon induction of differentiation, whereas only a nonsignificant but consistent small decrease in the levels of Cu in *Mtf1* KD proliferating myoblasts was detected (Fig. 8*F*). Then, we separated nuclear from cytosolic fractions in a similar way to the experiments shown in Fig. 6 and analyzed the levels of Cu in both fractions. Subcellular fractionation showed that *Mtf1* KD affected the nuclear Cu content. For instance, proliferating *Mtf1* KD myoblasts presented a nonsignificant decrease level of nuclear Cu compared to WT and *scr* controls, which was nevertheless recovered by overexpressing either the WT or MBS mutant versions of MTF1. Nuclear fractions of differentiating *Mtf1* KD cells showed a significant decrease in Cu content because KD myoblasts contained 50% less Cu compared to the control cells (Fig. 8*G*). A decrease in the cytosolic levels of proliferating and differentiating *Mtf1* KD myoblasts were also detected (Fig. 8*H*). Overall, the Cu levels were restored in the nuclear and cytosolic fractions by overexpressing the MTF1 WT protein but not by overexpressing the MBS mutant (Fig. 8*F*). As a control, we explored variations of Zn levels in these myoblasts. Studies from our laboratory have shown that the cellular levels of Zn during myogenesis are lower than for Cu (35, 42, 51, 105). In contrast to the results for Cu, we found that MTF1 depletion did not lead to a significant decrease in Zn levels in the nucleus or the cytoplasm of either proliferating or differentiating myoblasts (Supplemental Fig. S6). Expression of WT MTF1 or the MBS mutant in the *Mtf1* KD cells also did not significantly affect Zn levels in proliferating or differentiating cells (Supplemental Fig. S6). The results indicate that the effects of *Mtf1* KD on Cu levels are more significant than the effects on Zn levels and that the MBS mutation impacts than the ability of MTF1 to mediate effects of Cu while having little or no effect on the ability of MTF1 to mediate effects of Zn. These data suggest a role for MTF1 in mobilizing Cu into the nucleus during myogenesis. However, considering that MTF1 is a major regulator of the expression of a wide variety of chaperones and transporters (Fig. 2), it is plausible that the effect we observed here may be also a general consequence of the impact that MTF1 has over the network of cuproproteins. Thus, we do not overrule the possibility that other proteins are also part of this process.

Finally, taking into consideration our findings on the overall effect of *Mtf1* KD in myogenesis and the fact that MTF1 interacts with MyoD at myogenic promoters (Fig. 5), we asked whether the mutation of the MBS of MTF1 would impair the capabilities of MyoD to bind to myogenic promoters. We performed a ChIP–qRT-PCR analysis of myoblasts transduced with either the shRNA or the sgRNA against *Mtf1* and subsequently recovered with the WT or MBS mutant versions of MTF1. **Figure 9** shows that *Mtf1* KD impairs MyoD binding to the myogenin promoter. This effect is rescued by expressing WT MTF1 but

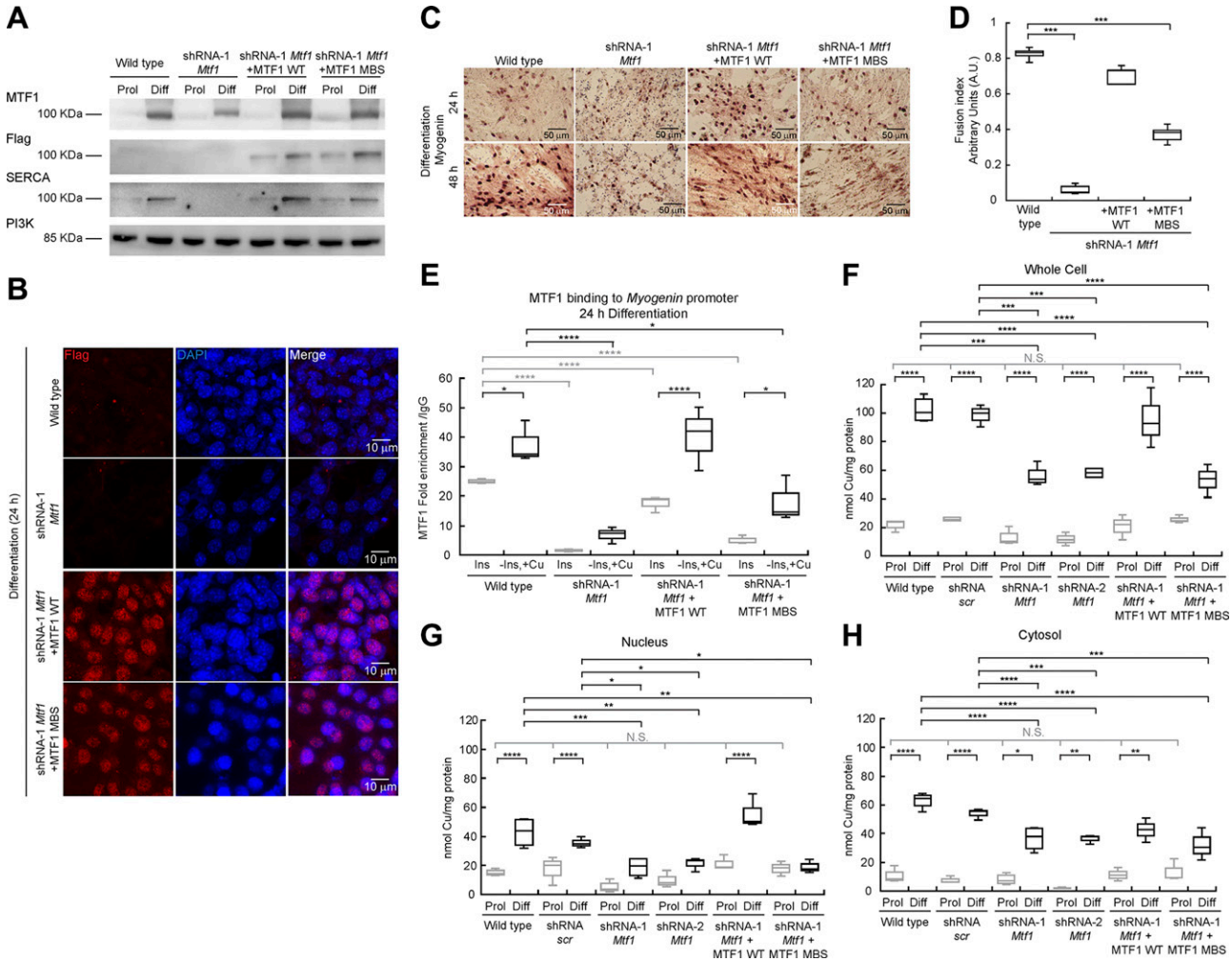

Figure 8. *Mtf1* phenotype is restored by MTF1 WT but partially recovered by the MBS mutant. *A*) Representative Western blot of primary myoblasts and myoblasts transduced with either *scr* shRNA or the shRNAs against *Mtf1*-1. The *Mtf1* shRNA-1 myoblasts were transduced with the MTF1 WT and MBS mutant. Samples were obtained for proliferation and 24 h after inducing differentiation. MTF1 levels were detected with the MTF1 antibody and the exogenous protein was detected with an anti-Flag antibody. SERCA levels were monitored as a differentiation marker. PI3K was used as loading control. *B*) Representative confocal microscopy images of differentiating primary myoblasts at 24 using an anti-Flag antibody to detect the localization of endogenous MTF1 (red) and DAPI (blue). *C*) Representative light micrographs of differentiating myoblasts immunostained for myogenin at 24 h. Images depicted in *A*–*C* are representative of ≥3 independent biologic experiments. *D*) Calculated fusion index for *Mtf1*-shRNA–transduced myoblasts and recovered with MTF1 WT or the MBS mutant; values for WT, and shRNA-1 MTF1 corresponds to the values shown in Fig. 2*E*. *E*) ChIP-qPCR for MTF1 binding to the *Myogenin* promoter in the myoblasts described in (*A*) differentiated with insulin or Cu. *F*) Whole cell Cu content of proliferating and differentiating primary myoblasts determined by AAS. *G*, *H*) Nuclear (*G*) and cytosolic (*H*) Cu content of proliferating and differentiating primary myoblasts. Metal determination was performed by AAS. Box plots represent the distribution of the data obtained from 3 independent biologic experiments ± SD. $^*P < 0.05$, $^{**}P < 0.01$, $^{***}P < 0.001$, $^{****}P \leq 0.0001$.

not or only partially restored by the MBS mutant protein (Fig. 9). These data further provide insights on the requirement for MTF1 to support myogenic gene expression.

DISCUSSION

There is a significant gap in our understanding of the roles that Cu plays in transcriptional regulation during mammalian development. Previous studies from our laboratory have shown that Cu promotes the proliferation and differentiation of primary myoblasts derived from mouse satellite cells (35). The pathways and mechanisms by which this transition metal induces this myogenic effect are largely unknown. In this work, we characterized the roles of Cu and the Cu-binding TF, MTF1, in myogenesis. Our data show that MTF1 expression is essential for myogenesis and that Cu enhances the expression of MTF1. Moreover, we have found that cellular Cu content influences the binding of MTF1 to target promoters. Finally, our studies revealed multiple mechanisms of MTF1 interaction at target genes, including direct binding to MREs and presumed indirect interactions through other TFs, including MyoD.

MTF1 is activated by different mechanisms to control metal and redox homeostasis, which include stimulation

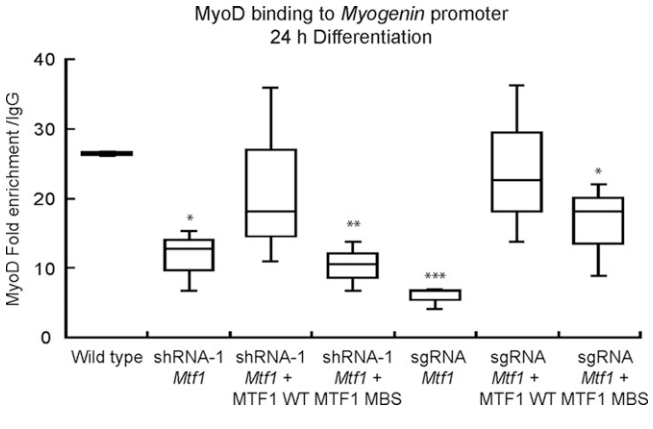

Figure 9. *MyoD* binding to the *Myogenin* promoter is decreased in differentiating myoblasts lacking MTF1 and is restored by MTF1 WT. ChIP-qPCR for MTF1 binding to the *Myogenin* promoter in differentiating primary myoblasts and myoblasts transduced with either the shRNA-1 or the sgRNA against *Mtf1*. The mutant myoblasts were then transduced with the MTF1 WT and MBS mutant. Box plots represent the distribution of the data obtained from 3 independent biologic experiments ± SD. $*P < 0.05$, $**P < 0.01$, $***P < 0.001$.

by cytosolic Zn and/or Zn released from MTs, or regulation by phosphorylation events (72, 74–78). On the other hand, the mechanisms by which MTF1 stimulates transcription of metal-responsive genes (MTs and metal transporters) in response to heavy metals and oxidative stress is well established. A characteristic of the promoters and enhancers of most of MTF1 target genes is the presence of MREs in the upstream regulatory sequences or just downstream of the TSS of metal-responsive genes that mediate MTF1 binding and regulation of gene expression (63, 70, 77, 83, 129). It is noteworthy that insulin supplementation in the culture medium is essential to induce myogenesis. In differentiating myoblasts, insulin activates signaling cascades such as PI3K and focal adhesion kinase (FAK) pathways, which enables myogenesis (88, 89). In the absence of this hormone, the myoblasts differentiate poorly (35). Therefore, our group has used this model to test the effect of Cu in skeletal muscle differentiation. In this work, we found that in myoblasts differentiated in the absence of insulin, the expression of MTF1 was decreased. This evidence points to a potential regulation of MTF1 expression and phosphorylation mediated by PI3K, and possibly other kinases, in the skeletal muscle lineage, which is in agreement with previous studies (78). Whether the activation of these kinases is regulated by Cu or Zn in the skeletal muscle lineage remains to be elucidated.

Activation of MTF1 by Cu has been investigated in several vertebrate models. Studies have addressed the expression of MT1 as an indirect measure of MTF1 activity upon stress induced by Cu and other metals. For instance, *in vivo* studies showing Cu-dependent changes in the transcription of *Mt1* in mouse liver showed that only high doses (over 5 mg/kg) of Cu administered to the animals induced the expression of this gene, whereas little effect of Cu was detected in the kidney (130). Studies in HeLa S3 cells showed that the transcript levels of *MtIIA* gene increased upon treatment with 300 μM $CuSO_4$. However, *in vitro* studies using whole cell extracts obtained from HeLa S3 cells exposed to 300 μM $CuSO_4$ failed to induce the MRE-binding activity, attributed to MTF1, although this concentration of Cu was able to induce the expression of metallothionein IIA (*mtIIA*) (131). In embryonic stem cells, induction of *Mt1* and *Mt2* was only achieved when the cells were treated with 500 μM $CuSO_4$ (66). It is noteworthy that studies from our laboratory showed that in differentiating, serum-deprived primary myoblasts derived from mouse satellite cells, concentrations over 100 μM are toxic to the cells (35). The data presented here showed that supplementation of differentiating myoblast with 30 μM $CuSO_4$, is sufficient to induce MTF1 expression and activation not only to drive the expression of metal-protective genes but also to promote the expression of myogenic genes. Overall, the data suggest that the cellular metal response and activation of MTF1 is dependent on the cell lineage. Studies from different laboratories suggest that Cu treatment is a poor activator of MTF1 in the context of its classic metal protective role, as shown by the expression of *Mt1*. However, the studies shown here suggest that low concentrations of Cu contribute to the activation of MTF1 in a novel role as a modulator of the expression of genes associated with myogenesis. Studies should be now directed to investigate the roles of MTF1 in the development of other lineages.

Additional roles for MTF1 have been proposed during embryonic development (57). MTF1 knockout leads to embryonic lethality at embryonic d 14 due to liver degeneration (57, 61). The MTF1 target genes *Mt1* and *Mt2* are constitutively and highly expressed in fetal liver (132–134), suggesting that these proteins are fundamental for liver development. However, deletions of both *Mt* genes had no effect in development under normal conditions, but mice were sensitive to Cd stress (135, 136). It is noteworthy that the MTF1 knockout murine model had no evidence of muscular phenotypes in developing embryos at E1 4 (57). These findings suggest that *1*) MTF1 contributes but is not required for muscle development; *2*) that MTF1 contributes to early muscle development but is only required for developmental stages at or after E14; or *3*) that there is an as yet unidentified redundancy for the roles of MTF1 in myogenesis. In addition, myogenic regulatory factors such as MYOD, myogenin, and the myocyte enhancer factor 2 have been shown to regulate the expression of MTF1 in differentiating myoblasts; however, no characterization has been done (137). Therefore, the specific roles for MTF1 in development and in lineage determination remain to be elucidated. Our work suggests 3 potential mechanisms for MTF1 binding to myogenic genes: *1*) Direct recognition and binding to MREs; *2*) indirect binding through additional TF binding sites; and *3*) indirect binding through MyoD binding sites.

Functional studies of the mammalian MTF1 showed a carboxy-terminal 13 aa domain that includes 4 conserved cysteines (CQCQCAC) that are necessary for MTF1 Zn and Cd sensing and transcriptional activation *in vivo* under moderate metal stress (138, 139). This cysteine cluster also mediates the homo-dimerization of MTF1, which is proposed to constitute a platform for the recruitment of additional transcriptional cofactors (140). In this regard,

Cu has been proposed to play a relevant role in stabilizing the dimer by constituting intermolecular disulphide bonds through oxidation of cysteines to further synergize with Zn to enhance transcription (140). However, the mechanistic role of this domain in regulation of metal homeostasis and development genes is not yet clear. Our data corroborate that Cu is internalized during myoblast differentiation and a fraction of the internalized Cu is relocalized to the nuclei. Considering the significant increase in MTF1 expression upon addition of Cu and the Cu-binding capabilities of the carboxy-terminal cysteine cluster of MTF1, it is plausible that MTF1 is partially responsible for the nuclear translocation of Cu observed in differentiating myoblasts. However, considering the effect of MTF1 KD on the expression of some cuproproteins, we cannot exclude the possibility that other Cu-binding proteins are involved in this process. This is supported by the partial recovery of the differentiation phenotype by the MBS mutant. Because myoblasts expressing the MBS mutant have basal levels of nuclear Cu, it is plausible that the partial differentiation observed might be due to other Cu-binding TFs or cytosolic Cu-binding proteins.

Current investigations in the field have been directed toward understanding the deleterious effects of Cu on the nervous system, liver, and intestine. However, little attention has been given to other organs and tissues, such as muscle, adipose, and bone. Strikingly, most of the systemic phenotypes observed in patients with Menkes and Wilson disease have been attributed to the neurologic damage that Cu exerts as a result from deficient systemic transport rather than a direct effect on the different tissues and organs. However, a complex developmental process such as myogenesis encompasses metabolic and morphologic changes linked to Cu-dependent energy production and redox homeostasis (1, 2). Our results shed light onto the importance of the function of Cu and MTF1 in the regulation of gene expression during developmental processes, such as skeletal muscle differentiation. A better understanding of how tissue Cu status affects growth and development at other cellular levels will be beneficial in the study of muscular phenotypes that present in diseases of Cu misbalance, such as Menkes and Wilson diseases. Fj

ACKNOWLEDGMENTS

The authors thank Courtney McCann, Dr. Sabriya Syed, Dr. Hanna Witwicka, and members of the T.P.-B. laboratory for insightful discussions regarding this manuscript. This work was supported by the Faculty Diversity Scholars Award from the University of Massachusetts Medical School to T.P.-B. Funding from the U.S. National Institute of Health [NIH; Grants R01GM56244 (National Institute of General Medical Sciences) to A.N.I. and R01HD072122 (Eunice Kennedy Shriver National Institute of Child Health and Human Development) to T.G.F.). S.J.V.G was supported by the University of Massachusetts Medical School funding for the Summer Undergraduate Research Experience Program [NIH Grant 2R25HL092610 (National Heart, Lung, and Blood Institute)]. Funding from the National Science Foundation [Division of Biological Infrastructure (DBI) 0959476 to J.G.N.]. S.J.H. is a Special Fellow of the Leukemia and Lymphoma Society. The authors declare no conflicts of interest.

AUTHOR CONTRIBUTIONS

T. Padilla-Benavides designed research; C. Tavera-Montañez, S. J. Hainer, D. Cangussu, S. J. V. Gordon, Y. Xiao, P. Reyes-Gutierrez, J. G. Navea, and T. Padilla-Benavides performed research; S. J. Hainer, A. N. Imbalzano, J. G. Navea, T. G. Fazzio, and T. Padilla-Benavides contributed reagents or analytic tools; S. J. Hainer, P. Reyes-Gutierrez, A. N. Imbalzano, J. G. Navea, T. G. Fazzio, and T. Padilla-Benavides analyzed data; C. Tavera-Montañez, S. J. Hainer, P. Reyes-Gutierrez, A. N. Imbalzano, and T. Padilla-Benavides wrote the paper.

REFERENCES

1. Fraústo da Silva, J. J. R., and Williams, R. J. P. (2001) *The Biological Chemistry of the Elements: The Inorganic Chemistry of Life*, Oxford University Press, Oxford, United Kingdom
2. Linder, M. C., and Hazegh-Azam, M. (1996) Copper biochemistry and molecular biology. *Am. J. Clin. Nutr.* **63**, 797S–811S
3. Festa, R. A., and Thiele, D. J. (2011) Copper: an essential metal in biology. *Curr. Biol.* **21**, R877–R883
4. Stadtman, E. R. (1993) Oxidation of free amino acids and amino acid residues in proteins by radiolysis and by metal-catalyzed reactions. *Annu. Rev. Biochem.* **62**, 797–821
5. Argüello, J. M., Raimunda, D., and Padilla-Benavides, T. (2013) Mechanisms of copper homeostasis in bacteria. *Front. Cell. Infect. Microbiol.* **3**, 73
6. Robinson, N. J., and Winge, D. R. (2010) Copper metallochaperones. *Annu. Rev. Biochem.* **79**, 537–562
7. Ohrvik, H., and Thiele, D. J. (2014) How copper traverses cellular membranes through the mammalian copper transporter 1, Ctr1. *Ann. N. Y. Acad. Sci.* **1314**, 32–41
8. Lutsenko, S., Barnes, N. L., Bartee, M. Y., and Dmitriev, O. Y. (2007) Function and regulation of human copper-transporting ATPases. *Physiol. Rev.* **87**, 1011–1046
9. Lutsenko, S., LeShane, E. S., and Shinde, U. (2007) Biochemical basis of regulation of human copper-transporting ATPases. *Arch. Biochem. Biophys.* **463**, 134–148
10. Barnes, N., Bartee, M. Y., Braiterman, L., Gupta, A., Ustiyan, V., Zuzel, V., Kaplan, J. H., Hubbard, A. L., and Lutsenko, S. (2009) Cell-specific trafficking suggests a new role for renal ATP7B in the intracellular copper storage. *Traffic* **10**, 767–779
11. Banci, L., Bertini, I., Cantini, F., and Ciofi-Baffoni, S. (2010) Cellular copper distribution: a mechanistic systems biology approach. *Cell. Mol. Life Sci.* **67**, 2563–2589
12. Liu, Y., Pilankatta, R., Hatori, Y., Lewis, D., and Inesi, G. (2010) Comparative features of copper ATPases ATP7A and ATP7B heterologously expressed in COS-1 cells. *Biochemistry* **49**, 10006–10012
13. Linz, R., and Lutsenko, S. (2007) Copper-transporting ATPases ATP7A and ATP7B: cousins, not twins. *J. Bioenerg. Biomembr.* **39**, 403–407
14. Barnes, N., Tsivkovskii, R., Tsivkovskaia, N., and Lutsenko, S. (2005) The copper-transporting ATPases, menkes and wilson disease proteins, have distinct roles in adult and developing cerebellum. *J. Biol. Chem.* **280**, 9640–9645
15. La Fontaine, S. L., Firth, S. D., Camakaris, J., Englezou, A., Theophilos, M. B., Petris, M. J., Howie, M., Lockhart, P. J., Greenough, M., Brooks, H., Reddel, R. R., and Mercer, J. F. (1998) Correction of the copper transport defect of Menkes patient fibroblasts by expression of the Menkes and Wilson ATPases. *J. Biol. Chem.* **273**, 31375–31380
16. Kaler, S. G. (1998) Diagnosis and therapy of Menkes syndrome, a genetic form of copper deficiency. *Am. J. Clin. Nutr.* **67** (Suppl), 1029S–1034S
17. Kodama, H., and Murata, Y. (1999) Molecular genetics and pathophysiology of Menkes disease. *Pediatr. Int.* **41**, 430–435
18. Kodama, H., Murata, Y., and Kobayashi, M. (1999) Clinical manifestations and treatment of Menkes disease and its variants. *Pediatr. Int.* **41**, 423–429
19. Strausak, D., Mercer, J. F., Dieter, H. H., Stremmel, W., and Multhaup, G. (2001) Copper in disorders with neurological

symptoms: Alzheimer's, Menkes, and Wilson diseases. *Brain Res. Bull.* **55**, 175–185
20. Uno, H., and Arya, S. (1987) Neuronal and vascular disorders of the brain and spinal cord in Menkes kinky hair disease. *Am. J. Med. Genet. Suppl.* **3**, 367–377
21. Van Wassenaer-van Hall, H. N. (1997) Neuroimaging in Wilson disease. *Metab. Brain Dis.* **12**, 1–19
22. Van Wassenaer-van Hall, H. N., van den Heuvel, A. G., Jansen, G. H., Hoogenraad, T. U., and Mali, W. P. (1995) Cranial MR in Wilson disease: abnormal white matter in extrapyramidal and pyramidal tracts. *AJNR Am. J. Neuroradiol.* **16**, 2021–2027
23. Ferenci, P. (2004) Review article: diagnosis and current therapy of Wilson's disease. *Aliment. Pharmacol. Ther.* **19**, 157–165
24. Gitlin, J. D. (2003) Wilson disease. *Gastroenterology* **125**, 1868–1877
25. Lutsenko, S. (2016) Copper trafficking to the secretory pathway. *Metallomics* **8**, 840–852
26. Siebert, X., Eipper, B. A., Mains, R. E., Prigge, S. T., Blackburn, N. J., and Amzel, L. M. (2005) The catalytic copper of peptidylglycine alpha-hydroxylating monooxygenase also plays a critical structural role. *Biophys. J.* **89**, 3312–3319
27. Vendelboe, T. V., Harris, P., Zhao, Y., Walter, T. S., Harlos, K., El Omari, K., and Christensen, H. E. (2016) The crystal structure of human dopamine β-hydroxylase at 2.9 Å resolution. *Sci. Adv.* **2**, e1500980
28. Csiszar, K. (2001) Lysyl oxidases: a novel multifunctional amine oxidase family. *Prog. Nucleic Acid Res. Mol. Biol.* **70**, 1–32
29. Karunadharma, P. P., Basisty, N., Chiao, Y. A., Dai, D. F., Drake, R., Levy, N., Koh, W. J., Emond, M. J., Kruse, S., Marcinek, D., Maccoss, M. J., and Rabinovitch, P. S. (2015) Respiratory chain protein turnover rates in mice are highly heterogeneous but strikingly conserved across tissues, ages, and treatments. *FASEB J.* **29**, 3582–3592
30. Ryall, J. G., Dell'Orso, S., Derfoul, A., Juan, A., Zare, H., Feng, X., Clermont, D., Koulnis, M., Gutierrez-Cruz, G., Fulco, M., and Sartorelli, V. (2015) The NAD(+)-dependent SIRT1 deacetylase translates a metabolic switch into regulatory epigenetics in skeletal muscle stem cells. *Cell Stem Cell* **16**, 171–183
31. Montarras, D., L'honoré, A., and Buckingham, M. (2013) Lying low but ready for action: the quiescent muscle satellite cell. *FEBS J.* **280**, 4036–4050
32. Remels, A. H., Langen, R. C., Schrauwen, P., Schaart, G., Schols, A. M., and Gosker, H. R. (2010) Regulation of mitochondrial biogenesis during myogenesis. *Mol. Cell. Endocrinol.* **315**, 113–120
33. Moyes, C. D., Mathieu-Costello, O. A., Tsuchiya, N., Filburn, C., and Hansford, R. G. (1997) Mitochondrial biogenesis during cellular differentiation. *Am. J. Physiol.* **272**, C1345–C1351
34. Merry, T. L., Steinberg, G. R., Lynch, G. S., and McConell, G. K. (2010) Skeletal muscle glucose uptake during contraction is regulated by nitric oxide and ROS independently of AMPK. *Am. J. Physiol. Endocrinol. Metab.* **298**, E577–E585
35. Vest, K. E., Paskavitz, A. L., Lee, J. B., and Padilla-Benavides, T. (2018) Dynamic changes in copper homeostasis and post-transcriptional regulation of Atp7a during myogenic differentiation. *Metallomics* **10**, 309–322
36. Gerber, A. N., Klesert, T. R., Bergstrom, D. A., and Tapscott, S. J. (1997) Two domains of MyoD mediate transcriptional activation of genes in repressive chromatin: a mechanism for lineage determination in myogenesis. *Genes Dev.* **11**, 436–450
37. De la Serna, I. L., Roy, K., Carlson, K. A., and Imbalzano, A. N. (2001) MyoD can induce cell cycle arrest but not muscle differentiation in the presence of dominant negative SWI/SNF chromatin remodeling enzymes. *J. Biol. Chem.* **276**, 41486–41491
38. De la Serna, I. L., Carlson, K. A., and Imbalzano, A. N. (2001) Mammalian SWI/SNF complexes promote MyoD-mediated muscle differentiation. *Nat. Genet.* **27**, 187–190
39. McKinsey, T. A., Zhang, C. L., and Olson, E. N. (2001) Control of muscle development by dueling HATs and HDACs. *Curr. Opin. Genet. Dev.* **11**, 497–504
40. Ohkawa, Y., Yoshimura, S., Higashi, C., Marfella, C. G., Dacwag, C. S., Tachibana, T., and Imbalzano, A. N. (2007) Myogenin and the SWI/SNF ATPase Brg1 maintain myogenic gene expression at different stages of skeletal myogenesis. *J. Biol. Chem.* **282**, 6564–6570
41. Padilla-Benavides, T., Nasipak, B. T., Paskavitz, A. L., Haokip, D. T., Schnabl, J. M., Nickerson, J. A., and Imbalzano, A. N. (2017) Casein kinase 2-mediated phosphorylation of Brahma-related gene 1 controls myoblast proliferation and contributes to SWI/SNF complex composition. *J. Biol. Chem.* **292**, 18592–18607
42. Paskavitz, A. L., Quintana, J., Cangussu, D., Tavera-Montañez, C., Xiao, Y., Ortiz-Miranda, S., Navea, J. G., and Padilla-Benavides, T. (2018) Differential expression of zinc transporters accompanies the differentiation of C2C12 myoblasts. *J. Trace Elem. Med. Biol.* **49**, 27–34
43. Fujisawa-Sehara, A., Hanaoka, K., Hayasaka, M., Hiromasa-Yagami, T., and Nabeshima, Y. (1993) Upstream region of the myogenin gene confers transcriptional activation in muscle cell lineages during mouse embryogenesis. *Biochem. Biophys. Res. Commun.* **191**, 351–356
44. Rudnicki, M. A., Schnegelsberg, P. N., Stead, R. H., Braun, T., Arnold, H. H., and Jaenisch, R. (1993) MyoD or Myf-5 is required for the formation of skeletal muscle. *Cell* **75**, 1351–1359
45. Megeney, L. A., and Rudnicki, M. A. (1995) Determination versus differentiation and the MyoD family of transcription factors. *Biochem. Cell. Biol.* **73**, 723–732
46. Venuti, J. M., Morris, J. H., Vivian, J. L., Olson, E. N., and Klein, W. H. (1995) Myogenin is required for late but not early aspects of myogenesis during mouse development. *J. Cell Biol.* **128**, 563–576
47. Rudnicki, M. A., and Jaenisch, R. (1995) The MyoD family of transcription factors and skeletal myogenesis. *BioEssays* **17**, 203–209
48. Megeney, L. A., Kablar, B., Garrett, K., Anderson, J. E., and Rudnicki, M. A. (1996) MyoD is required for myogenic stem cell function in adult skeletal muscle. *Genes Dev.* **10**, 1173–1183
49. Friday, B. B., Mitchell, P. O., Kegley, K. M., and Pavlath, G. K. (2003) Calcineurin initiates skeletal muscle differentiation by activating MEF2 and MyoD. *Differentiation* **71**, 217–227
50. Berkes, C. A., and Tapscott, S. J. (2005) MyoD and the transcriptional control of myogenesis. *Semin. Cell Dev. Biol.* **16**, 585–595
51. Gordon, S. J. V., Fenker, D. E., Vest, K. E., and Padilla-Benavides, T. (2019) Manganese influx and expression of ZIP8 is essential in primary myoblasts and contributes to activation of SOD2. *Metallomics* **11**, 1140–1153
52. Muller, P. A., and Klomp, L. W. (2009) ATOX1: a novel copper-responsive transcription factor in mammals? *Int. J. Biochem. Cell Biol.* **41**, 1233–1236
53. Yuan, S., Chen, S., Xi, Z., and Liu, Y. (2017) Copper-finger protein of Sp1: the molecular basis of copper sensing. *Metallomics* **9**, 1169–1175
54. Itoh, S., Kim, H. W., Nakagawa, O., Ozumi, K., Lessner, S. M., Aoki, H., Akram, K., McKinney, R. D., Ushio-Fukai, M., and Fukai, T. (2008) Novel role of antioxidant-1 (Atox1) as a copper-dependent transcription factor involved in cell proliferation. *J. Biol. Chem.* **283**, 9157–9167
55. Jeney, V., Itoh, S., Wendt, M., Gradek, Q., Ushio-Fukai, M., Harrison, D. G., and Fukai, T. (2005) Role of antioxidant-1 in extracellular superoxide dismutase function and expression. *Circ. Res.* **96**, 723–729
56. Balamurugan, K., Egli, D., Selvaraj, A., Zhang, B., Georgiev, O., and Schaffner, W. (2004) Metal-responsive transcription factor (MTF-1) and heavy metal stress response in Drosophila and mammalian cells: a functional comparison. *Biol. Chem.* **385**, 597–603
57. Günes, C., Heuchel, R., Georgiev, O., Müller, K. H., Lichtlen, P., Blüthmann, H., Marino, S., Aguzzi, A., and Schaffner, W. (1998) Embryonic lethality and liver degeneration in mice lacking the metal-responsive transcriptional activator MTF-1. *EMBO J.* **17**, 2846–2854
58. Günther, V., Lindert, U., and Schaffner, W. (2012) The taste of heavy metals: gene regulation by MTF-1. *Biochim. Biophys. Acta* **1823**, 1416–1425
59. Rutherford, J. C., and Bird, A. J. (2004) Metal-responsive transcription factors that regulate iron, zinc, and copper homeostasis in eukaryotic cells. *Eukaryot. Cell* **3**, 1–13
60. Selvaraj, A., Balamurugan, K., Yepiskoposyan, H., Zhou, H., Egli, D., Georgiev, O., Thiele, D. J., and Schaffner, W. (2005) Metal-responsive transcription factor (MTF-1) handles both extremes, copper load and copper starvation, by activating different genes. *Genes Dev.* **19**, 891–896
61. Wang, Y., Wimmer, U., Lichtlen, P., Inderbitzin, D., Stieger, B., Meier, P. J., Hunziker, L., Stallmach, T., Forrer, R., Rülicke, T., Georgiev, O., and Schaffner, W. (2004) Metal-responsive transcription factor-1 (MTF-1) is essential for embryonic liver development and heavy metal detoxification in the adult liver. *FASEB J.* **18**, 1071–1079
62. Gilmour, J., Assi, S. A., Jaegle, U., Kulu, D., van de Werken, H., Clarke, D., Westhead, D. R., Philipsen, S., and Bonifer, C. (2014) A crucial role for the ubiquitously expressed transcription factor Sp1 at early stages of hematopoietic specification. *Development* **141**, 2391–2401

63. Green, C. J., Lichtlen, P., Huynh, N. T., Yanovsky, M., Laderoute, K. R., Schaffner, W., and Murphy, B. J. (2001) Placenta growth factor gene expression is induced by hypoxia in fibroblasts: a central role for metal transcription factor-1. *Cancer Res.* **61**, 2696–2703
64. Seo, S. J., Kim, H. T., Cho, G., Rho, H. M., and Jung, G. (1996) Sp1 and C/EBP-related factor regulate the transcription of human Cu/Zn SOD gene. *Gene* **178**, 177–185
65. Song, I. S., Chen, H. H., Aiba, I., Hossain, A., Liang, Z. D., Klomp, L. W., and Kuo, M. T. (2008) Transcription factor Sp1 plays an important role in the regulation of copper homeostasis in mammalian cells. *Mol. Pharmacol.* **74**, 705–713
66. Heuchel, R., Radtke, F., Georgiev, O., Stark, G., Aguet, M., and Schaffner, W. (1994) The transcription factor MTF-1 is essential for basal and heavy metal-induced metallothionein gene expression. *EMBO J.* **13**, 2870–2875
67. Potter, B. M., Feng, L. S., Parasuram, P., Matskevich, V. A., Wilson, J. A., Andrews, G. K., and Laity, J. H. (2005) The six zinc fingers of metal-responsive element binding transcription factor-1 form stable and quasi-ordered structures with relatively small differences in zinc affinities. *J. Biol. Chem.* **280**, 28529–28540
68. Zhang, B., Egli, D., Georgiev, O., and Schaffner, W. (2001) The Drosophila homolog of mammalian zinc finger factor MTF-1 activates transcription in response to heavy metals. *Mol. Cell. Biol.* **21**, 4505–4514
69. Giedroc, D. P., Chen, X., and Apuy, J. L. (2001) Metal response element (MRE)-binding transcription factor-1 (MTF-1): structure, function, and regulation. *Antioxid. Redox Signal.* **3**, 577–596
70. Stuart, G. W., Searle, P. F., Chen, H. Y., Brinster, R. L., and Palmiter, R. D. (1984) A 12-base-pair DNA motif that is repeated several times in metallothionein gene promoters confers metal regulation to a heterologous gene. *Proc. Natl. Acad. Sci. USA* **81**, 7318–7322
71. Stuart, G. W., Searle, P. F., and Palmiter, R. D. (1985) Identification of multiple metal regulatory elements in mouse metallothionein-I promoter by assaying synthetic sequences. *Nature* **317**, 828–831
72. Murphy, B. J., Andrews, G. K., Bittel, D., Discher, D. J., McCue, J., Green, C. J., Yanovsky, M., Giaccia, A., Sutherland, R. M., Laderoute, K. R., and Webster, K. A. (1999) Activation of metallothionein gene expression by hypoxia involves metal response elements and metal transcription factor-1. *Cancer Res.* **59**, 1315–1322
73. Li, Y., Kimura, T., Laity, J. H., and Andrews, G. K. (2006) The zinc-sensing mechanism of mouse MTF-1 involves linker peptides between the zinc fingers. *Mol. Cell. Biol.* **26**, 5580–5587
74. Saydam, N., Georgiev, O., Nakano, M. Y., Greber, U. F., and Schaffner, W. (2001) Nucleo-cytoplasmic trafficking of metal-regulatory transcription factor 1 is regulated by diverse stress signals. *J. Biol. Chem.* **276**, 25487–25495
75. Ruttkay-Nedecky, B., Nejdl, L., Gumulec, J., Zitka, O., Masarik, M., Eckschlager, T., Stiborova, M., Adam, V., and Kizek, R. (2013) The role of metallothionein in oxidative stress. *Int. J. Mol. Sci.* **14**, 6044–6066
76. LaRochelle, O., Gagné, V., Charron, J., Soh, J. W., and Séguin, C. (2001) Phosphorylation is involved in the activation of metal-regulatory transcription factor 1 in response to metal ions. *J. Biol. Chem.* **276**, 41879–41888
77. Larochelle, O., Stewart, G., Moffatt, P., Tremblay, V., and Séguin, C. (2001) Characterization of the mouse metal-regulatory-element-binding proteins, metal element protein-1 and metal regulatory transcription factor-1. *Biochem. J.* **353**, 591–601
78. Andéol, Y., Bonneau, J., M Gagné, L., Jacquet, K., Rivest, V., Huot, M. É., and Séguin, C. (2018) The phosphoinositide 3-kinase pathway and glycogen synthase kinase-3 positively regulate the activity of metal-responsive transcription factor-1 in response to zinc ions. *Biochem. Cell Biol.* **96**, 726–733
79. Lynes, M. A., Kang, Y. J., Sensi, S. L., Perdrizet, G. A., and Hightower, L. E. (2007) Heavy metal ions in normal physiology, toxic stress, and cytoprotection. *Ann. N. Y. Acad. Sci.* **1113**, 159–172
80. Miles, A. T., Hawksworth, G. M., Beattie, J. H., and Rodilla, V. (2000) Induction, regulation, degradation, and biological significance of mammalian metallothioneins. *Crit. Rev. Biochem. Mol. Biol.* **35**, 35–70
81. Park, J. D., Liu, Y., and Klaassen, C. D. (2001) Protective effect of metallothionein against the toxicity of cadmium and other metals (1). *Toxicology* **163**, 93–100
82. Andrews, G. K., Lee, D. K., Ravindra, R., Lichtlen, P., Sirito, M., Sawadogo, M., and Schaffner, W. (2001) The transcription factors MTF-1 and USF1 cooperate to regulate mouse metallothionein-I expression in response to the essential metal zinc in visceral endoderm cells during early development. *EMBO J.* **20**, 1114–1122
83. Langmade, S. J., Ravindra, R., Daniels, P. J., and Andrews, G. K. (2000) The transcription factor MTF-1 mediates metal regulation of the mouse ZnT1 gene. *J. Biol. Chem.* **275**, 34803–34809
84. Lichten, L. A., Liuzzi, J. P., and Cousins, R. J. (2009) Interleukin-1beta contributes via nitric oxide to the upregulation and functional activity of the zinc transporter Zip14 (Slc39a14) in murine hepatocytes. *Am. J. Physiol. Gastrointest. Liver Physiol.* **296**, G860–G867
85. Sims, H. I., Chirn, G. W., and Marr II, M. T. (2012) Single nucleotide in the MTF-1 binding site can determine metal-specific transcription activation. *Proc. Natl. Acad. Sci. USA* **109**, 16516–16521
86. Chen, X., Hua, H., Balamurugan, K., Kong, X., Zhang, L., George, G. N., Georgiev, O., Schaffner, W., and Giedroc, D. P. (2008) Copper sensing function of Drosophila metal-responsive transcription factor-1 is mediated by a tetranuclear Cu(I) cluster. *Nucleic Acids Res.* **36**, 3128–3138
87. Nasipak, B. T., Padilla-Benavides, T., Green, K. M., Leszyk, J. D., Mao, W., Konda, S., Sif, S., Shaffer, S. A., Ohkawa, Y., and Imbalzano, A. N. (2015) Opposing calcium-dependent signalling pathways control skeletal muscle differentiation by regulating a chromatin remodelling enzyme. *Nat. Commun.* **6**, 7441
88. Conejo, R., and Lorenzo, M. (2001) Insulin signaling leading to proliferation, survival, and membrane ruffling in C2C12 myoblasts. *J. Cell. Physiol.* **187**, 96–108
89. Goel, H. L., and Dey, C. S. (2002) Focal adhesion kinase tyrosine phosphorylation is associated with myogenesis and modulated by insulin. *Cell Prolif.* **35**, 131–142
90. Sanjana, N. E., Shalem, O., and Zhang, F. (2014) Improved vectors and genome-wide libraries for CRISPR screening. *Nat. Methods* **11**, 783–784
91. Shalem, O., Sanjana, N. E., Hartenian, E., Shi, X., Scott, D. A., Mikkelson, T., Heckl, D., Ebert, B. L., Root, D. E., Doench, J. G., and Zhang, F. (2014) Genome-scale CRISPR-Cas9 knockout screening in human cells. *Science* **343**, 84–87
92. Guidi, C. J., Veal, T. M., Jones, S. N., and Imbalzano, A. N. (2004) Transcriptional compensation for loss of an allele of the Ini1 tumor suppressor. *J. Biol. Chem.* **279**, 4180–4185
93. Pear, W. S., Nolan, G. P., Scott, M. L., and Baltimore, D. (1993) Production of high-titer helper-free retroviruses by transient transfection. *Proc. Natl. Acad. Sci. USA* **90**, 8392–8396
94. Livak, K. J., and Schmittgen, T. D. (2001) Analysis of relative gene expression data using real-time quantitative PCR and the 2(-Delta Delta C(T)) Method. *Methods* **25**, 402–408
95. Heinz, S., Benner, C., Spann, N., Bertolino, E., Lin, Y. C., Laslo, P., Cheng, J. X., Murre, C., Singh, H., and Glass, C. K. (2010) Simple combinations of lineage-determining transcription factors prime cis-regulatory elements required for macrophage and B cell identities. *Mol. Cell* **38**, 576–589
96. Soleimani, V. D., Yin, H., Jahani-Asl, A., Ming, H., Kockx, C. E., van Ijcken, W. F., Grosveld, F., and Rudnicki, M. A. (2012) Snail regulates MyoD binding-site occupancy to direct enhancer switching and differentiation-specific transcription in myogenesis. *Mol. Cell* **47**, 457–468
97. Tripathi, S., Pohl, M. O., Zhou, Y., Rodriguez-Frandsen, A., Wang, G., Stein, D. A., Moulton, H. M., DeJesus, P., Che, J., Mulder, L. C., Yángüez, E., Andenmatten, D., Pache, L., Manicassamy, B., Albrecht, R. A., Gonzalez, M. G., Nguyen, Q., Brass, A., Elledge, S., White, M., Shapira, S., Hacohen, N., Karlas, A., Meyer, T. F., Shales, M., Gatorano, A., Johnson, J. R., Jang, G., Johnson, T., Verschueren, E., Sanders, D., Krogan, N., Shaw, M., König, R., Stertz, S., García-Sastre, A., and Chanda, S. K. (2015) Meta- and orthogonal integration of influenza "OMICs" data defines a role for UBR4 in virus budding. *Cell Host Microbe* **18**, 723–735
98. Hatzis, P., and Talianidis, I. (2002) Dynamics of enhancer-promoter communication during differentiation-induced gene activation. *Mol. Cell* **10**, 1467–1477
99. Kouskouti, A., and Talianidis, I. (2005) Histone modifications defining active genes persist after transcriptional and mitotic inactivation. *EMBO J.* **24**, 347–357
100. Harikrishnan, K. N., Chow, M. Z., Baker, E. K., Pal, S., Bassal, S., Brasacchio, D., Wang, L., Craig, J. M., Jones, P. L., Sif, S., and El-Osta, A. (2005) Brahma links the SWI/SNF chromatin-remodeling complex with MeCP2-dependent transcriptional silencing. *Nat. Genet.* **37**, 254–264
101. Bradford, M. M. (1976) A rapid and sensitive method for the quantitation of microgram quantities of protein utilizing the principle of protein-dye binding. *Anal. Biochem.* **72**, 248–254

102. Suzuki, K., Bose, P., Leong-Quong, R. Y., Fujita, D. J., and Riabowol, K. (2010) REAP: a two minute cell fractionation method. *BMC Res. Notes* **3**, 294
103. Cheng, L., Wang, F., Shou, H., Huang, F., Zheng, L., He, F., Li, J., Zhao, F. J., Ueno, D., Ma, J. F., and Wu, P. (2007) Mutation in nicotianamine aminotransferase stimulated the Fe(II) acquisition system and led to iron accumulation in rice. *Plant Physiol.* **145**, 1647–1657
104. Raimunda, D., Padilla-Benavides, T., Vogt, S., Boutigny, S., Tomkinson, K. N., Finney, L. A., and Argüello, J. M. (2013) Periplasmic response upon disruption of transmembrane Cu transport in Pseudomonas aeruginosa. *Metallomics* **5**, 144–151
105. Gordon, S. J. V., Xiao, Y., Paskavitz, A. L., Navarro-Tito, N., Navea, J. G., and Padilla-Benavides, T. (2019) Atomic absorbance spectroscopy to measure intracellular zinc pools in mammalian cells. *J. Vis. Exp.* **157**, e59519
106. Studier, F. W. (2005) Protein production by auto-induction in high density shaking cultures. *Protein Expr. Purif.* **41**, 207–234
107. Raimunda, D., Long, J. E., Padilla-Benavides, T., Sassetti, C. M., and Argüello, J. M. (2014) Differential roles for the Co(2+) /Ni(2+) transporting ATPases, CtpD and CtpJ, in Mycobacterium tuberculosis virulence. *Mol. Microbiol.* **91**, 185–197
108. Padilla-Benavides, T., and Argüello, J. M. (2016) Assay of copper transfer and binding to P1B-ATPases. *Methods Mol. Biol.* **1377**, 267–277
109. Padilla-Benavides, T., George Thompson, A. M., McEvoy, M. M., and Argüello, J. M. (2014) Mechanism of ATPase-mediated Cu+ export and delivery to periplasmic chaperones: the interaction of Escherichia coli CopA and CusF. *J. Biol. Chem.* **289**, 20492–20501
110. Padilla-Benavides, T., McCann, C. J., and Argüello, J. M. (2013) The mechanism of Cu^+ transport ATPases: interaction with CU^+ chaperones and the role of transient metal-binding sites. *J. Biol. Chem.* **288**, 69–78
111. Günther, V., Waldvogel, D., Nosswitz, M., Georgiev, O., and Schaffner, W. (2012) Dissection of Drosophila MTF-1 reveals a domain for differential target gene activation upon copper overload vs. copper starvation. *Int. J. Biochem. Cell Biol.* **44**, 404–411
112. Bittel, D., Dalton, T., Samson, S. L., Gedamu, L., and Andrews, G. K. (1998) The DNA binding activity of metal response element-binding transcription factor-1 is activated in vivo and in vitro by zinc, but not by other transition metals. *J. Biol. Chem.* **273**, 7127–7133
113. Bittel, D. C., Smirnova, I. V., and Andrews, G. K. (2000) Functional heterogeneity in the zinc fingers of metalloregulatory protein metal response element-binding transcription factor-1. *J. Biol. Chem.* **275**, 37194–37201
114. Saydam, N., Steiner, F., Georgiev, O., and Schaffner, W. (2003) Heat and heavy metal stress synergize to mediate transcriptional hyperactivation by metal-responsive transcription factor MTF-1. *J. Biol. Chem.* **278**, 31879–31883
115. Lichtlen, P., and Schaffner, W. (2001) Putting its fingers on stressful situations: the heavy metal-regulatory transcription factor MTF-1. *BioEssays* **23**, 1010–1017
116. Saini, N., Georgiev, O., and Schaffner, W. (2011) The parkin mutant phenotype in the fly is largely rescued by metal-responsive transcription factor (MTF-1). *Mol. Cell. Biol.* **31**, 2151–2161
117. Conejo, R., Valverde, A. M., Benito, M., and Lorenzo, M. (2001) Insulin produces myogenesis in C2C12 myoblasts by induction of NF-kappaB and downregulation of AP-1 activities. *J. Cell. Physiol.* **186**, 82–94
118. Scarpulla, R. C. (2011) Metabolic control of mitochondrial biogenesis through the PGC-1 family regulatory network. *Biochim. Biophys. Acta* **1813**, 1269–1278
119. Kelly, D. P., and Scarpulla, R. C. (2004) Transcriptional regulatory circuits controlling mitochondrial biogenesis and function. *Genes Dev.* **18**, 357–368
120. Cao, Y., Yao, Z., Sarkar, D., Lawrence, M., Sanchez, G. J., Parker, M. H., MacQuarrie, K. L., Davison, J., Morgan, M. T., Ruzzo, W. L., Gentleman, R. C., and Tapscott, S. J. (2010) Genome-wide MyoD binding in skeletal muscle cells: a potential for broad cellular reprogramming. *Dev. Cell* **18**, 662–674
121. Himeda, C. L., Ranish, J. A., Pearson, R. C., Crossley, M., and Hauschka, S. D. (2010) KLF3 regulates muscle-specific gene expression and synergizes with serum response factor on KLF binding sites. *Mol. Cell. Biol.* **30**, 3430–3443
122. Yokoyama, S., Ito, Y., Ueno-Kudoh, H., Shimizu, H., Uchibe, K., Albini, S., Mitsuoka, K., Miyaki, S., Kiso, M., Nagai, A., Hikata, T., Osada, T., Fukuda, N., Yamashita, S., Harada, D., Mezzano, V., Kasai, M., Puri, P. L., Hayashizaki, Y., Okado, H., Hashimoto, M., and Asahara, H. (2009) A systems approach reveals that the myogenesis genome network is regulated by the transcriptional repressor RP58. *Dev. Cell* **17**, 836–848
123. Yokoyama, S., and Asahara, H. (2011) The myogenic transcriptional network. *Cell. Mol. Life Sci.* **68**, 1843–1849
124. Mitchell, D. L., and DiMario, J. X. (2010) Bimodal, reciprocal regulation of fibroblast growth factor receptor 1 promoter activity by BTEB1/KLF9 during myogenesis. *Mol. Biol. Cell* **21**, 2780–2787
125. Hasty, P., Bradley, A., Morris, J. H., Edmondson, D. G., Venuti, J. M., Olson, E. N., and Klein, W. H. (1993) Muscle deficiency and neonatal death in mice with a targeted mutation in the myogenin gene. *Nature* **364**, 501–506
126. Nabeshima, Y., Hanaoka, K., Hayasaka, M., Esumi, E., Li, S., Nonaka, I., and Nabeshima, Y. (1993) Myogenin gene disruption results in perinatal lethality because of severe muscle defect. *Nature* **364**, 532–535
127. Huovila, A. P., Turner, A. J., Pelto-Huikko, M., Kärkkäinen, I., and Ortiz, R. M. (2005) Shedding light on ADAM metalloproteinases. *Trends Biochem. Sci.* **30**, 413–422
128. Lassar, A. B., Buskin, J. N., Lockshon, D., Davis, R. L., Apone, S., Hauschka, S. D., and Weintraub, H. (1989) MyoD is a sequence-specific DNA binding protein requiring a region of myc homology to bind to the muscle creatine kinase enhancer. *Cell* **58**, 823–831
129. Cramer, M., Nagy, I., Murphy, B. J., Gassmann, M., Hottiger, M. O., Georgiev, O., and Schaffner, W. (2005) NF-kappaB contributes to transcription of placenta growth factor and interacts with metal responsive transcription factor-1 in hypoxic human cells. *Biol. Chem.* **386**, 865–872
130. Durnam, D. M., and Palmiter, R. D. (1981) Transcriptional regulation of the mouse metallothionein-I gene by heavy metals. *J. Biol. Chem.* **256**, 5712–5716
131. Murata, M., Gong, P., Suzuki, K., and Koizumi, S. (1999) Differential metal response and regulation of human heavy metal-inducible genes. *J. Cell. Physiol.* **180**, 105–113
132. Kern, S. R., Smith, H. A., Fontaine, D., and Bryan, S. E. (1981) Partitioning of zinc and copper in fetal liver subfractions: appearance of metallothionein-like proteins during development. *Toxicol. Appl. Pharmacol.* **59**, 346–354
133. Ouellette, A. J. (1982) Metallothionein mRNA expression in fetal mouse organs. *Dev. Biol.* **92**, 240–246
134. Quaife, C., Hammer, R. E., Mottet, N. K., and Palmiter, R. D. (1986) Glucocorticoid regulation of metallothionein during murine development. *Dev. Biol.* **118**, 549–555
135. Michalska, A. E., and Choo, K. H. (1993) Targeting and germ-line transmission of a null mutation at the metallothionein I and II loci in mouse. *Proc. Natl. Acad. Sci. USA* **90**, 8088–8092
136. Masters, B. A., Kelly, E. J., Quaife, C. J., Brinster, R. L., and Palmiter, R. D. (1994) Targeted disruption of metallothionein I and II genes increases sensitivity to cadmium. *Proc. Natl. Acad. Sci. USA* **91**, 584–588
137. Blais, A., Tsikitis, M., Acosta-Alvear, D., Sharan, R., Kluger, Y., and Dynlacht, B. D. (2005) An initial blueprint for myogenic differentiation. *Genes Dev.* **19**, 553–569
138. Chen, X., Zhang, B., Harmon, P. M., Schaffner, W., Peterson, D. O., and Giedroc, D. P. (2004) A novel cysteine cluster in human metal-responsive transcription factor 1 is required for heavy metal-induced transcriptional activation in vivo. *J. Biol. Chem.* **279**, 4515–4522
139. He, X., and Ma, Q. (2009) Induction of metallothionein I by arsenic via metal-activated transcription factor 1: critical role of C-terminal cysteine residues in arsenic sensing. *J. Biol. Chem.* **284**, 12609–12621
140. Günther, V., Davis, A. M., Georgiev, O., and Schaffner, W. (2012) A conserved cysteine cluster, essential for transcriptional activity, mediates homodimerization of human metal-responsive transcription factor-1 (MTF-1). *Biochim. Biophys. Acta* **1823**, 476–483

Received for publication June 28, 2019.
Accepted for publication September 23, 2019.